JVSTA
JOURNAL OF VACUUM SCIENCE AND TECHNOLOGY A

Tobacco mosaic virus: A biological building block for micro/nano/bio systems

Xiao Z. Fan, Ekaterina Pomerantseva, Markus Gnerlich, Adam Brown, Konstantinos Gerasopoulos et al.

Citation: J. Vac. Sci. Technol. A **31**, 050815 (2013); doi: 10.1116/1.4816584
View online: http://dx.doi.org/10.1116/1.4816584
View Table of Contents: http://avspublications.org/resource/1/JVTAD6/v31/i5
Published by the AVS: Science & Technology of Materials, Interfaces, and Processing

Related Articles

Recent search for new superhard materials: Go nano!
J. Vac. Sci. Technol. A 31, 050822 (2013)

Advances in silicon carbide science and technology at the micro- and nanoscales
J. Vac. Sci. Technol. A 31, 050805 (2013)

Three dimensional reciprocal space measurement by x-ray diffraction using linear and area detectors: Applications to texture and defects determination in oriented thin films and nanoprecipitates
J. Vac. Sci. Technol. A 31, 021505 (2013)

The Si3N4/TiN Interface: 3. Si3N4/TiN(001) Grown with a −150 V Substrate Bias and Analyzed In situ using Angle-resolved X-ray Photoelectron Spectroscopy
Surf. Sci. Spectra 19, 52 (2012)

Facile fabrication of scalable patterned nickel nanocone arrays for field emission applications
J. Vac. Sci. Technol. B 31, 02B104 (2013)

Additional information on J. Vac. Sci. Technol. A

Journal Homepage: http://avspublications.org/jvsta
Journal Information: http://avspublications.org/jvsta/about/about_the_journal
Top downloads: http://avspublications.org/jvsta/top_20_most_downloaded
Information for Authors: http://avspublications.org/jvsta/authors/information_for_contributors

ADVERTISEMENT

REVIEW ARTICLE

Tobacco mosaic virus: A biological building block for micro/nano/bio systems

Xiao Z. Fan,[a] Ekaterina Pomerantseva,[a] and Markus Gnerlich[a]
MEMS Sensors and Actuators Laboratory (MSAL), Department of Electrical and Computer Engineering, University of Maryland, College Park, Maryland 20742 and Institute for Systems Research, University of Maryland, College Park, Maryland 20742

Adam Brown
Fischell Department of Bioengineering, University of Maryland, College Park, Maryland 20742 and Institute for Bioscience and Biotechnology Research, University of Maryland, College Park, Maryland 20742

Konstantinos Gerasopoulos
MEMS Sensors and Actuators Laboratory (MSAL), Department of Electrical and Computer Engineering, University of Maryland, College Park, Maryland 20742 and Institute for Systems Research, University of Maryland, College Park, Maryland 20742

Matthew McCarthy
Department of Mechanical Engineering and Mechanics, Drexel University, Philadelphia, Pennsylvania 19104

James Culver
Institute for Bioscience and Biotechnology Research and Department of Plant Sciences and Landscape Architecture, University of Maryland, College Park, Maryland 20742

Reza Ghodssi[b]
MEMS Sensors and Actuators Laboratory (MSAL), Department of Electrical and Computer Engineering, University of Maryland, College Park, Maryland 20742, Fischell Department of Bioengineering, University of Maryland, College Park, Maryland 20742, and Institute for Systems Research, University of Maryland, College Park, Maryland 20742

(Received 11 March 2013; accepted 24 June 2013; published 5 August 2013)

Tobacco mosaic virus (TMV) has the potential to be an ideal candidate for a building block of the next-generation micro/nano/bio systems. The TMV virion is a high-aspect ratio rigid nanotube that is robust and compatible with some conventional microfabrication processes. TMV can be chemically and genetically modified to enhance its physical properties and tailor them to specific applications. This review covers the use of TMV nanostructures in a wide range of micro/nano/bio systems. TMV has been utilized in the production of nanowires, nanostructured thin films, biomimetic surfaces, novel sensors, high performance microbatteries, solid-state electronics, and engineered biosystems. The work highlighted here is meant to give a perspective of the entire breadth of the properties of these virions, from their synthesis and functionalization to assembly and patterning, as well as feature works that represent key milestones in the field of biofabrication and biomaterial integration. The advantages already demonstrated by the integration of TMV nanostructures, even at this early stage of development, suggest that the applications for this micro/nano/bio systems building block will continue to grow. © *2013 American Vacuum Society*.
[http://dx.doi.org/10.1116/1.4816584]

I. INTRODUCTION

The MEMS field is constantly evolving, enabling more effective miniaturization of functional devices and integrated systems. However, fundamental limitations in microfabrication technology do not allow scaling down beyond certain limits. Integration of nanostructured materials into functional microdevices remains a challenging goal that cannot be achieved in many cases by standard processing methods, confining them to the research stages of prototype development. This is mainly due to processing limitations and integration incompatibilities. Semiconductor nanostructures, offering zero to three-dimensional nanomaterials, take advantage of traditional semiconductor processing techniques to realize nanostructures that possess unique properties. Some of the most common processes used involve vapor–liquid–solid reactions through the combination of catalytic particles on a substrate and chemical vapor deposition or epitaxial methods.[1–5] Other less expensive techniques such as hydrothermal synthesis,[6,7] thermal evaporation,[8] sol–gel processes,[9,10] and electrodeposition[11] have also been reported. Although all of these techniques have

[a]X. Z. Fan, E. Pomerantseva, and M. Gnerlich contributed equally to this work.
[b]Author to whom correspondence should be addressed; electronic mail: ghodssi@umd.edu

demonstrated significant progress in the field, they often have to balance control over structural properties, variability of yield, and alignment of structures with cost of synthesis, equipment performance, and process compatibility with remaining processing steps.

Nanofabrication techniques based on the use of self-assembling biomolecules represent an alternative approach that has recently been extensively studied for the fabrication of nanometer-scale devices. Bionanomaterials utilize biological building blocks to realize nanostructures. These techniques demonstrate fine control over the size and shape of the biotemplated particles. In addition, selective patterning of biomolecules is often possible, enabling the fabrication of the desired device architectures. Their characteristic traits, compared to that of semiconductors, include enhanced structural and functional versatility, self-assembly onto surfaces and tunability for tailored applications. These benefits are combined with the low cost involved in synthesis and processing and a wealth of information provided by the fields of biology and bioengineering. DNA,[12–17] peptides,[18] bacteria,[18–21] and proteins[22] have all been used to fabricate various nanostructures, including nanofibers, nanoparticles, and quantum dots. These synthetic pathways show diversity and great promise to replace semiconductor approaches for certain application specific niches.

One category of biological nanostructures that offers unique functional expressions is plant and bacteria viruses. These particles consist of macromolecular assemblies of nucleic acid packaged by many copies of coat proteins (CPs). In addition to their surface-exposed functional groups that facilitate chemical reactions, these molecules display some unique advantages: they exhibit exceptional stability in a wide range of temperatures and *p*H values while at the same time withstanding treatment in denaturing organic solvent–water mixtures.[23] Among the available viruses, *Tobacco mosaic virus* (TMV) is one of the most extensively studied filamentous structures for nanoscale applications (Fig. 1). Properties of TMV rods that are particularly useful for the integration of nanobiomaterials with microsystems and devices are (1) the known three-dimensional structure of TMV and four related virus strains,[24–27] (2) a wealth of biophysical information on the self-assembly characteristics of TMV on various substrates,[28] (3) the availability of a full-length infectious cDNA clone of the virus that allows the creation of novel virus structures and surfaces via established genetic modification techniques,[29,30] (4) a wide range of existing coat protein variants with diverse assembly properties,[31] (5) the ability to easily purify large quantities of viruses and coat proteins from infected plants,[32–34] and (6) the structural robustness which makes it compatible with conventional microfabrication techniques.[32,35,36]

Tobacco has been cultivated over a long history in the United States. More recently, Tobacco (*Nicotiana tabacum* L.) a herbaceous perennial has been investigated as a biomass crop for the production of proteins and vaccines.[37] Tobacco cultivation is well suited for high cropping densities (40 000 plants/acre) and multiple (4–5) harvests per season. Studies have shown that 25–30 tons of wet biomass can be obtained from an acre of tobacco grown at a cost of about $175 dollars per wet ton.[38] A routine purification process can produce ca. 0.5 g of purified TMV per pound of wet tobacco tissue. Thus, it is possible to grow kilogram quantities of virus per acre of tobacco at an extremely low cost. Commercial scale virus-particle purification would be relatively simple and could involve tissue homogenization by press or blender, heating and *p*H 5.0 extraction to remove plant cell components, followed by clarification using disk stacked centrifugation and final purification by ultrafiltration. Thus, the additional costs derived from particle purification would also be low.

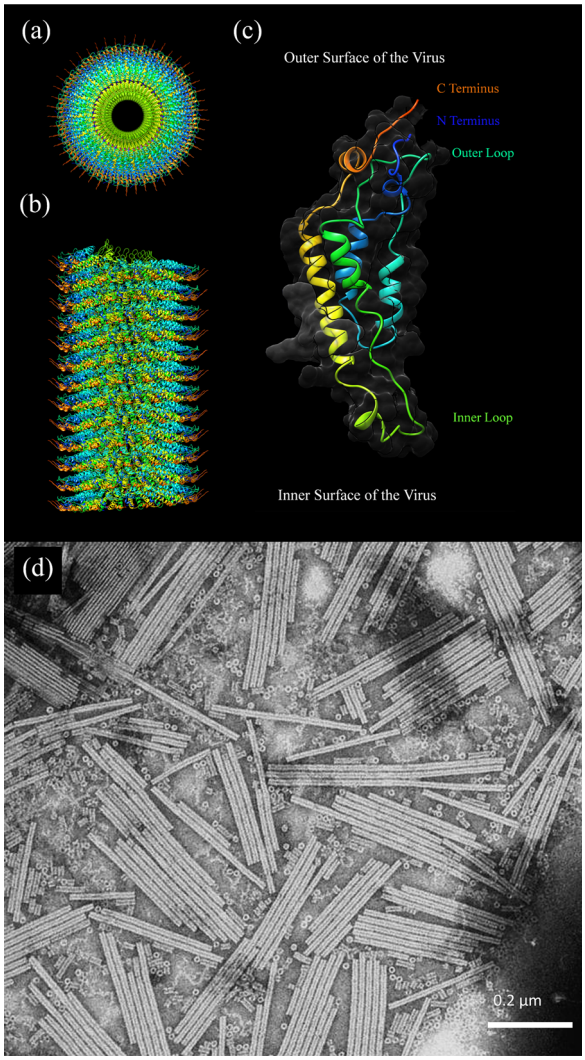

FIG. 1. (Color online) TMV structure: (a, b) Molecular model showing the top and side view of a TMV virion. (c) A ribbon diagram of a single coat protein subunit. (d) A TEM image of wild-type TMV image courtesy of Tomas Moravec.

The applications of TMV for microsystems are surveyed and summarized in this review. Numerous resources are available that describe TMV from the biologic perspective, but the information on its application and integration with devices from an engineer's perspective is limited yet highly appealing. The process of synthesis and purification of TMV nanorods, various virus assembly and patterning techniques, different material coatings methods, and finally the use of

TMV in sensors, energy storage, and electronic devices are described in detail. By reviewing the past discoveries and understanding today's developments, we hope to generate excitement and inspiration for the next generation of devices and systems.

II. *TOBACCO MOSAIC VIRUS* STRUCTURE AND GENETIC MODIFICATIONS

To research the techniques for the laboratory-scale integration of TMV into devices, large quantities of the virus can be generated by infecting, incubating and purifying it from tobacco (*Nicotiana tabacum*) plants.[31,33,39,40] Both purified wild-type TMV as well as stable genetically modified forms of the virus can be easily harvested from infected plants. It is important to discuss the structure and chemical properties of TMV to better understand its role in constructing functional microsystems.

The virus structure (Fig. 1) is a hollow rod-shaped tube, 3000 Å long and 180 Å in outer diameter, with an inner diameter of 40 Å. The length of the encapsidated genomic ribonucleic acid (RNA) limits the length of the virus rod, terminating at the 3′- and 5′-ends. Each virus has ca. 2130 identical CP subunits surrounding a single strand of RNA. The molecular weight of the coat protein unit is 17.5 kDa, and it forms a helix with a pitch of 23 Å with $16\frac{1}{3}$ coat proteins per turn. The structure of the TMV virion has been resolved at a resolution of 2.9 Å using X-ray diffraction.[24] Each CP molecule is composed of a chain of 158 amino acids that are folded into four main alpha-helices which are connected by inner and outer loops [Fig. 1(c)]. The inner radius of the molecule, lining the inner channel, consists of a long and a short inner loop. The outer radius of the CP molecule, lining the outer surface of the virion, displays the N and C termini of the amino acid chain.

The availability of a full-length complementary cDNA clone of the TMV genome coupled with the well-established tertiary structure of the coat protein and its architecture of assembly allows for specific targeted alteration of virion surface properties. Coat protein modifications are typically made by inserting peptides consisting of 2–20 amino acids, or replacing an amino acid with the corresponding amine.[29–31] On the external surface of the assembled virion, potential locations for desired modifications include both the N and C termini (Figs. 1 and 2) and the surface loop between two alpha-helices of the coat protein. On the surface of the inner channel, modifications are limited to the long loop lining the inner channel. A list of genetically modified TMV for micro/nano/bio systems applications is summarized in Table I.

Large peptide modifications to the CP may cause failure of virus assembly due to steric hindrance. It is possible to use genetic approaches to prevent this type of failure and allow appropriate virus assembly.[41] Genetically modified coat proteins may also require alternative purification processes to accommodate the modifications. For example, cysteine (Cys) modifications require the addition of dithiothreitol (DTT) to the virus extraction buffer to break up disulfide bonds that are likely to form between free thiol ends. This severs the attractions between parallel TMV-1Cys rods, preventing viruses from clustering into bundles.

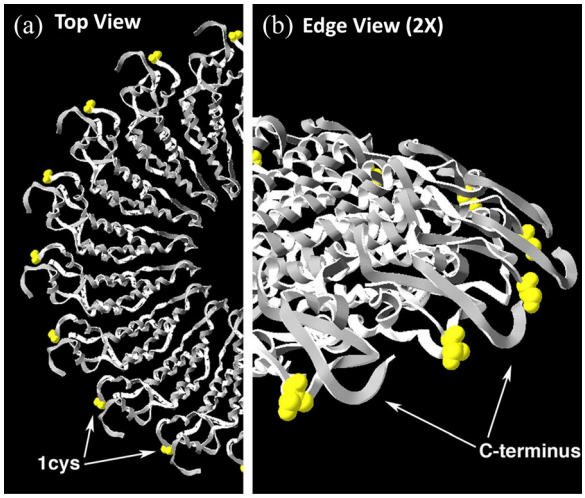

FIG. 2. (Color online) CAD drawing showing the structural location of the TMV-1Cys mutation. (a) A top down view showing coat proteins of half a turn within the TMV rod and (b) 2× magnification of an edge view for the same single turn (location of the cysteine mutation on the n-terminus is highlighted in spherical representation). Reprinted with permission from K. Gerasopoulos, M. McCarthy, E. Royston, J. N. Culver, and R. Ghodssi, J. Micromech. Microeng. **18**(10), 104003 (2008). Copyright 2007, IOP Publishing.

The binding densities of maleimide–fluorescein to cysteines in TMV-1Cys and NHS-ester–fluorescein to lysines in TMV-1Lys were monitored by fluorescent microscopy.[42] The number of fluorescein molecules bound to each TMV-1Cys and TMV-1Lys was ca. 1850 and ca. 1400, corresponding to a loading density of ca. 85% and 65%, respectively. Matrix-assisted laser desorption/ionization time-of-flight mass spectrometry (MALDI-TOF MS) of TMV-1Cys and TMV-1Lys bound with fluorescein verified that a fraction of mutated coat proteins did not undergo fluorescein binding. It was hypothesized that NHS-ester is larger than maleimide, which caused a steric hindrance to the fluorescein binding and led to a larger portion of unbound coat proteins. A smaller molecule, propargyl maleimide, was used to bind to TMV-1Cys and showed no unbound coat proteins in MALDI-TOF MS, suggesting that cysteine is present in every CP which is important for utilization of cysteine binding properties.

An alternative to genetically modifying the coat protein sequence is to functionalize the surface chemically, post purification. For example, fluorescent tags can be labeled onto the surface of TMV-1Cys, taking advantage of the available thiol bonds.[34,43,44] Bruckman *et al.*[45] demonstrated that oligo-aniline (OANI) motifs were capable of being labeled onto the TMV surface (TMV:OANI) using a three step bioconjugation protocol by attaching terminal alkynes to phenol side chains of TMV CP. Dimethyl sulfoxide can be added to the solution as a cosolvent to decrease reaction between OANI units, preventing aggregation and bundling of TMV:OANI, similar in purpose to DTT addition to the TMV-1Cys solution.

TABLE I. TMV conjugations for micro/nano/bio systems applications.

Mutation name	Modification	Location	Reference
TMV-1Cys	Cysteine	N terminus	63
TMV-2Cys	2 × Cysteine	N terminus	59
TMV-1Lys	Lysine	N terminus	42
E50Q	Glutamic acid to glutamine	Position 50	33
E95Q/D109N	Glutamic acid to glutamine; aspartic acid to asparagine	Position 95 and 109, respectively	57
TMV-TNT	TNT specific peptide, Cysteine	N and C terminus	41

Wild-type TMV is highly robust and it can withstand temperatures up to 50 °C for 30 min, *p*H level 5–8, and even in organic solvent–water mixtures.[23] There are a few reports that TMV can also withstand harsher conditions.[46] TMV mutated derivatives are generally handled and suspended in milder conditions, typically 0.1M *p*H 7 phosphate buffer solutions at room temperature. These conditions are observed for most applications reported in this article unless otherwise specified. Viruses can also be re-suspended in or dialyzed with deionized water if phosphate buffer is undesirable.[47] TMV and their derivatives are generally stored at −15 °C for prolonged periods of time. Repetition of thawing and refreezing of the sample should be kept to a minimum since that can decrease the lifetime of the suspension. However, TMV's structure and functionality can be preserved for months to years under ideal storage conditions, adding to TMV's capability to be an attractive building block module for constructing microsystems. A systematic study on the viability of conjugated viruses in different conditions has not been reported to the authors' knowledge. Different mutations to the virus CP structure are believed to require a different operating condition ranges.

III. FUNCTIONAL COATINGS OF *TOBACCO MOSAIC VIRUS*

Nanoscale metal and metal oxide particles offer unique catalytic, electronic, and sensing properties. Fabrication of homogeneous nanoparticle assemblies as well as nanowires, with the potential to selectively pattern them onto predetermined positions, is important for the development of next-generation microdevices. TMV-based synthesis of inorganic materials offers a possibility to manufacture structures with the controlled size, shape, and position at nanoscale. In this section we discuss coating of TMV nanotemplates with various materials, which is an important step toward integration of nanostructured materials in functional devices.

A. Metal coating

The exterior surface and/or the central channel of TMV has been selectively metallized using electroless deposition (ELD).[47–57] ELD is advantageous for biological structures since they cannot be contacted electrically; therefore, electrodeposition cannot be utilized. In addition, ELD usually provides uniform coating even on high-aspect ratio structures including nanoscale elements. In the first step, the surface of the TMV particle is activated with noble metal nanoparticles produced by decomposition of Pt(II) or Pd(II) complexes. Then the TMV suspension is mixed with ELD solution containing metal ions, complexants, and a reductant. The deposition is first catalyzed by the noble metal nanoparticles and then proceeds autocatalytically. Therefore, the metal particles continue to grow.

The selectivity for the inner or exterior surface coating can be controlled by the presence or absence of phosphate ions in the TMV suspension.[47] The exterior surface of the wild-type TMV coat protein predominantly consists of oxygen-containing groups (such as hydroxyl and carboxylate), while inside the inner channel, amine, primary amide,

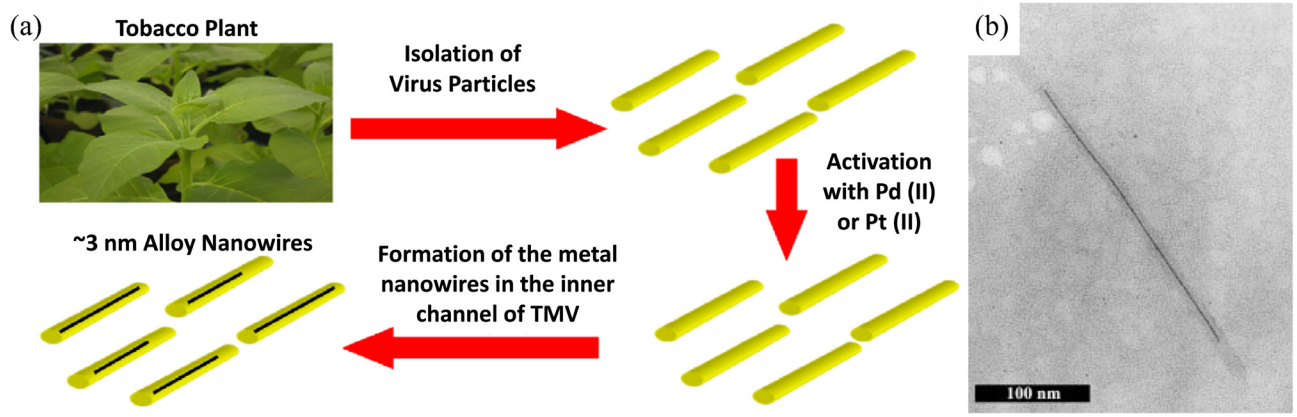

FIG. 3. (Color online) (a) Schematic presentation of the synthesis of metallic nanowires in the inner channel of TMV particle. Adapted from Ref. 53. (b) TEM image of a single virion containing a ca. 250 nm long nickel wire inside the inner TMV channel. Reprinted with permission from M. Knez, M. Sumser, A. M. Bittner, C. Wege, H. Jeske, T. P. Martin, and K. Kern, Adv. Funct. Mater. **14**(2), 116 (2004). Copyright 2004, WILEY-VCH Verlag GmbH & Co. KGaA.

and guanidyl groups prevail. To coat the inner channel with metals, the virions were dialyzed against water prior to activation and metallization, in order to remove Na/K phosphate buffer. As a result, in the absence of phosphate ions (Fig. 3), no metal particles form on the exterior virus surface in the ELD bath. In addition, hydrogen bubbles, which evolve during metallization, may prevent the formation of metal clusters on the exterior virus surface. The metal clusters grow inside the inner channel forming up to 600 nm long metal nanowires (although generally nanowires with the length of ca. 100–200 nm are formed). Pure metal (Ag,[57] Ni, Co,[49] Cu,[51] Pt (Ref. 52) and alloy (Co/Fe,[53] Fe/Pt,[56] Co/Pt (Ref. 58) nanowires of 3–4 nm in diameter were synthesized in the central channel of TMV. An example of a ca. 250 nm long nickel nanowire is shown in Fig. 3(b). Silver nanowires were grown inside the genetically modified TMV mutant—E95Q/D109N.[57] To be used in nanoelectronics, metal nanowires can be isolated from the biological shell by decomposition in oxygen plasma.

When phosphate ions are present, they attach to the outer viral surface, promoting the selective reduction of metal ions during surface activation step and in the ELD baths. In this case ELD yields larger clusters of metals exclusively on the outer surface of TMV (Fig. 4). When wild-type TMV is used for metallization in the presence of phosphate ions, metal clusters deposit on the outer virus surface without forming homogeneous films.[47,49,54,55] When a TMV suspension is treated with $PdCl_4^-$ and a reducing agent is added, the exterior surface of TMV is coated with a palladium layer.[47] Deposition of platinum on the TMV outer surface was achieved in solutions containing $PtCl_6^{2-}$. The length of the activation step was suggested to play an important role. For different activation times, different morphology of the metal layers was observed (few small particles versus coalesced particles forming a layer).[55] Nickel and cobalt coatings, which consisted of large intergrown particles, are shown in Figs. 4(d) and 4(e).

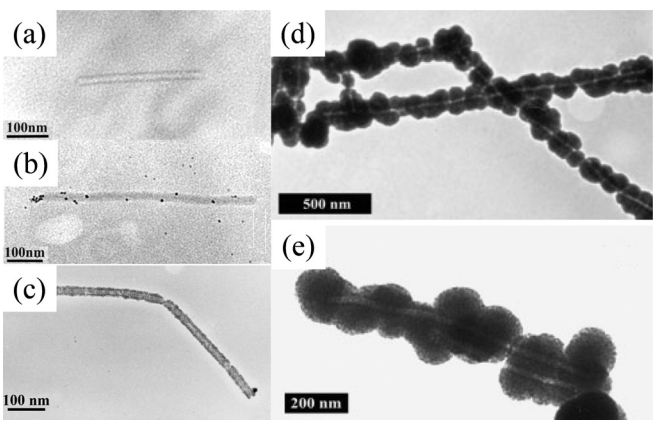

FIG. 4. TEM images of (a) a TMV particle (only the contours appear dark; the coat proteins and the central channel are transparent); (b) a TMV after Pd(II) adsorption (activation), followed by reduction. Reprinted with permission from M. Knez, A. M. Bittner, F. Boes, C. Wege, H. Jeske, E. Maiβ, and K. Kern, Nano Lett. **3**(8), 1079 (2003). Copyright 2003, American Chemical Society; (c) two TMVs densely covered with palladium particles; (d, e) Pt(II) pretreated TMVs metallized with (d) nickel and (e) cobalt. Reprinted with permission from M. Knez, M. Sumser, A. M. Bittner, C. Wege, H. Jeske, T. P. Martin, and K. Kern, Adv. Funct. Mater. **14**(2), 116 (2004). Copyright 2004, WILEY-VCH Verlag GmbH & Co. KGaA.

Micro-/nanoscale device fabrication that uses solution chemistry processes and biotemplates requires uniform inorganic coatings on biological molecules over the entire surface. However, when the size of the target coating surface is reduced to the nanometer scale, controlling the uniformity becomes challenging. As it was discussed above, when wild-type TMV was used, metal salt reduction resulted in inefficient, discrete and irregular metal nucleation on the virions (Fig. 4), due to the random nucleation site formations on the virion surface. Maintaining a uniform and continuous coating on the entire biotemplate surface remains a fundamental challenge in biotemplate-based inorganic materials synthesis. Introduction of Cys residues, containing thiol groups, onto TMV surface enhances metal binding ability. The strong covalent bond between thiol groups and metals has made thiol coupling an effective method for achieving uniform metal coatings on TMV surface. TMV-1Cys and TMV-2Cys mutants were used to coat virus with Au,[59,60] Ag,[59] Pd,[59–61] and Au/Pd.[62] Improved metal cluster deposition forming more uniform coating was observed compared to the wild-type TMV.

The genetically engineered TMV-1Cys mutant exhibits self-assembly on gold surfaces with a preferential vertical orientation via gold–thiol interaction,[32,36,63] which is discussed in detail in Sec. IV. Such self-assembled TMV-1Cys virion particles functioned as robust templates for the deposition of nickel and cobalt, producing porous 3D metalized networks of oriented metal-coated virus particles.[63] A schematic of self-assembly and metal coating processes is shown in Fig. 5(a). For TMV self-assembly, gold-coated substrates are held in a suspension containing TMV-1Cys molecules for 1–2 days. Afterwards, the surface of TMV is activated with palladium catalyst followed by nickel (or cobalt) ELD reaction. Due to the autocatalytic nature of Ni (or Co) plating, a uniform metal coating around TMV is formed. The morphology of the metalized self-assembled TMV molecules is shown in Figs. 5(b) and 5(c). Near vertical attachment of the virus rods is achieved [Fig. 5(d)]. The metal layer is rigid and can be used for electrodes applications.[36,63] In addition, Ni (or Co)-coated virus-assembled nanoforests produce almost an order of magnitude increase in surface area compared to planar structures. If after TMV-1Cys binding, the chips are rinsed and dried, this drying step causes virus particles to lose vertical orientation. Further metal coating steps result in the formation of preferentially horizontally oriented TMV-1Cys-templated metalized particles on a chip surface, as it was demonstrated for palladium coatings (Fig. 6).[64–66]

B. Metal oxide coating

Only a few examples of TMV coating with materials other than metals exist in the literature.[33,67–69] For example, a genetically modified TMV mutant, E50Q, was used for silica coating on the virus outer surface. SiO_2 was formed by

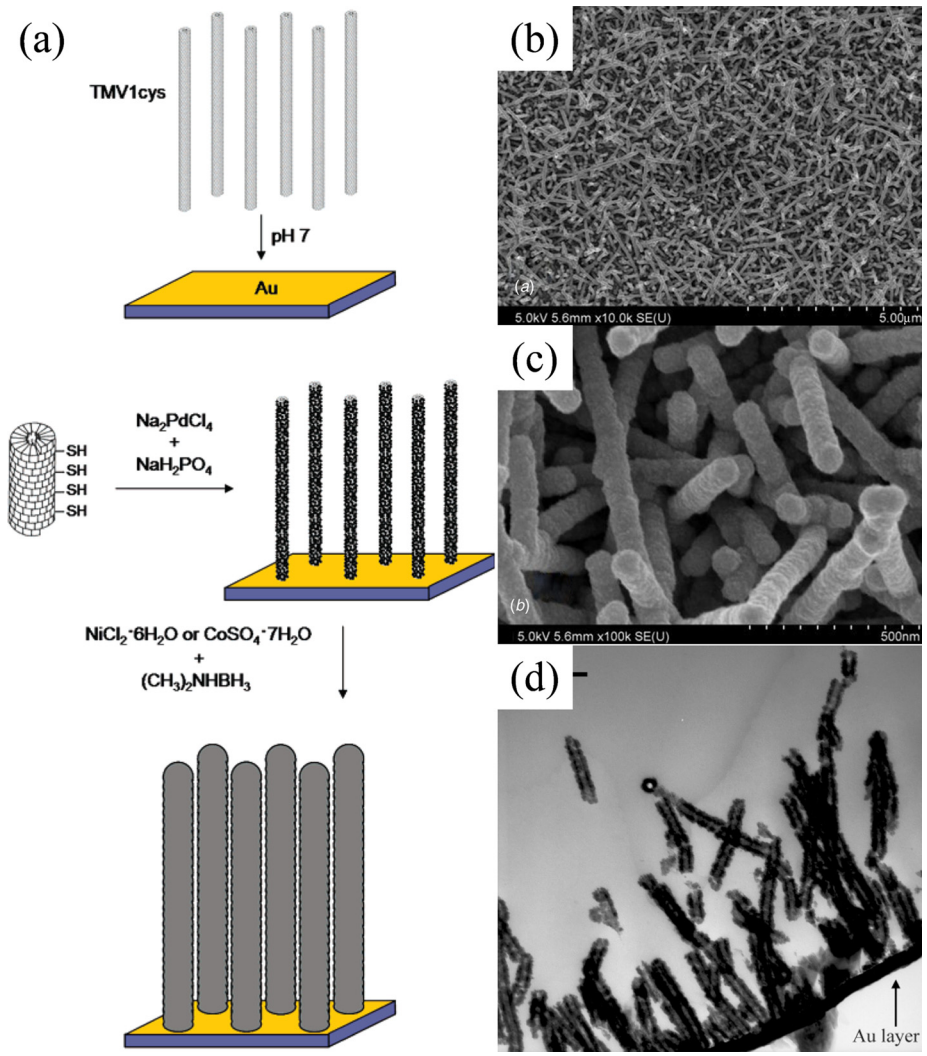

FIG. 5. (Color online) (a) Diagram for the assembly of nickel- and cobalt-coated TMV-1Cys templates attached to a gold surface. Reprinted with permission from E. Royston, A. Ghosh, P. Kofinas, M. T. Harris, and J. N. Culver, Langmuir **24**(3), 906 (2008). Copyright 2008. American Chemical Society. (b, c) SEM images at two magnifications of nickel-coated TMV self-assembled nanostructures. Reprinted with permission from K. Gerasopoulos, M. McCarthy, E. Royston, J. N. Culver, and R. Ghodssi, J. Micromech. Microeng. **18**(10), 104003 (2008). Copyright 2007, IOP Publishing. (d) TEM image showing a cross section of nickel-coated TMV-1Cys attached perpendicular to a gold-coated surface. Reprinted with permission from E. Royston, A. Ghosh, P. Kofinas, M. T. Harris, and J. N. Culver, Langmuir **24**(3), 906 (2008). Copyright 2008, American Chemical Society.

hydrolysis and condensation reaction of tetra-ethyl-ortho-silicate (TEOS) in aqueous methanolic solution in a $p\mathrm{H} > 7$.[33] Interestingly, virus particles remained stable in alcohol–water solution (with water concentration $\geq 40\%$), although alcohols generally denature proteins. The robustness of TMV under such harsh conditions highlights its usefulness as a template for the synthesis of nanostructures.

Atomic layer deposition (ALD) is a thin-film materials synthesis method providing the unique ability to produce uniform coating with high degree of control on nanostructured, high surface area substrates. During the ALD process, precursor doses are sequentially pulsed in the chamber. This leads to self-limiting adsorption/reaction on a substrate surface, in the ideal case with a monolayer control. The result is a material film built layer by layer.[70–74] Deposition of materials at temperatures below 100 °C creates opportunities to utilize ALD for the coating of temperature-sensitive biological particles, such as TMV. For example, using ALD, TMV was coated with Al_2O_3 and TiO_2.[67] Coating of both exterior surface and inner channel surface was achieved as shown in Fig. 7. In several cases, a hollow metal oxide tube inside the viral channel was observed. These results show the potential of ALD for the coating of biological biomolecules. Channels less than 4 nm in diameter can be accessed by the precursors and nanotubes can be fabricated.[67]

Zinc oxide coating on the TMV surface was first achieved by activation of the virus surface with Pd(II) and a subsequent ZnO nucleation during electroless deposition.[69] Uniform ZnO nanowires with precisely controlled coating thickness were synthesized on TMV particles immobilized on silicon substrates from aqueous alkaline solution without an activation step. The coating consisted of closely packed spherical polycrystalline ZnO nanoparticles. This ZnO deposition process can be repeated to achieve thicker coatings. The comparison of untreated TMV with TMV particles after one and five deposition cycles is shown in Fig. 8.[68]

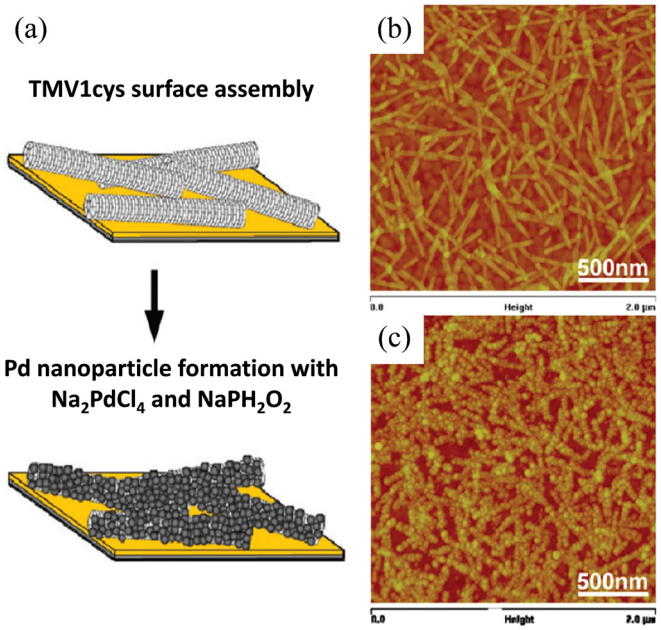

FIG. 6. (Color online) (a) Schematic diagram representing TMV-1Cys horizontal assembly onto gold surfaces followed by reductive metallization of the Pd precursor. (b) AFM image of surface-assembled TMV-1Cys on a gold chip. (c) AFM image of Pd nanoparticles formed on surface-assembled TMV-1Cys. Reprinted with permission from A. K. Manocchi, S. Seifert, B. Lee, and H. Yi, Langmuir **26**(10), 7516 (2010). Copyright 2010, American Chemical Society.

C. Multilayer coatings

Sequential coating of nanoparticles with materials of unique properties can create core/shell structures exhibiting multiple functionalities, which is important for device performance. Multilayer coatings on the exterior TMV surface can be created using various strategies. For example, SiO_2/Pt coatings were achieved on wild-type TMV following previously described processes.[75] A TEOS-based bath was used for silica deposition.[33] Platinum metallization was achieved in K_2PtCl_4 solution. When this was followed by placing SiO_2/Pt-coated TMV particles in the TEOS-based bath again, a second SiO_2 layer was deposited on top, forming a SiO_2/Pt/SiO_2 structure.

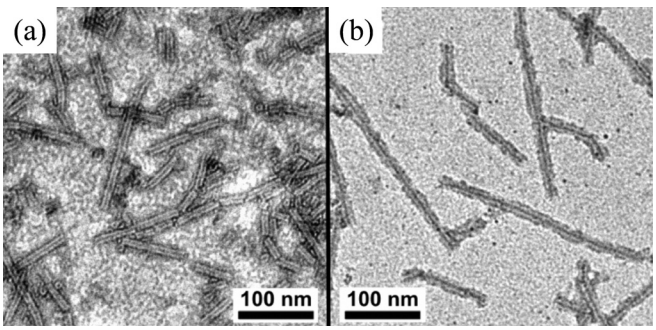

FIG. 7. (a) TEM image of TMV treated with TiO_2 by ALD. (b) After ultrasonication the TiO_2 is partially removed from the outer surface and mainly the inner channel of the TMV remains covered with TiO_2. Reprinted with permission from M. Knez, A. Kadri, C. Wege, U. Gösele, H. Jeske, and K. Nielsch, Nano Lett. **6**(6), 1172 (2006). Copyright 2006, American Chemical Society.

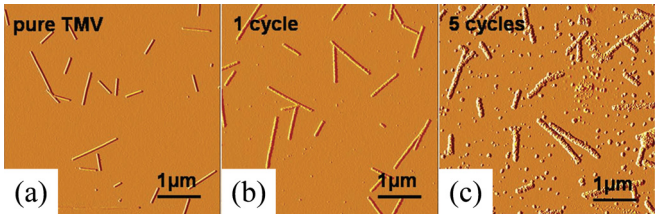

FIG. 8. (Color online) AFM amplitude images of ZnO-mineralized TMV nanowires on silicon substrates. The nanowire thickness increases with the number of the deposited cycles. Reprinted with permission from P. Atanasova, D. Rothenstein, J. J. Schneider, R. C. Hoffmann, S. Dilfer, S. Eiben, C. Wege, H. Jeske, and J. Bill, Adv. Mater. **23**(42), 4918 (2011). Copyright 2004, WILEY-VCH Verlag GmbH & Co. KGaA.

Another example of multilayered coating was demonstrated using Ni-coated TMV-1Cys self-assembled nanoforests.[32,35,76–80] The nickel plating process can be combined with conformal thin-film deposition techniques, such as atomic layer deposition, sputtering, and electrodeposition, and creates core/shell nanocomposites with a highly conductive nickel core and various other materials deposited on top. A library of such core/shell nanostructures has been successfully developed, including the following shell materials: Si (sputtering, electrodeposition),[76,77] Sn (electrodeposition),[78] TiO_2,[35] V_2O_5,[80] and Al_2O_3 (Refs. 32 and 79) (ALD). Figure 9 shows an example of a single TMV-1Cys/Ni/Al_2O_3 nanocomposite particle. EDS line-scan elemental mapping of Ni, Al, and O revealed the Ni peak located at the center of the Al and O peaks. Similar core/shell structures were obtained for other materials and they can be used as a starting point in designing strategies for incorporation of biological templates into functional devices for energy storage, catalysis, and sensing.

IV. ASSEMBLY, POSITIONING, AND PATTERNING

The ability to assemble and pattern the TMV into functional structures is critical to make use of the virus' unique properties. Although the morphology and assembly process of the virus itself have been extensively studied,[24,81–84] the research covered here is concerned with TMV enhanced by non-natural properties. TMV is a versatile template and it can be geometrically organized using special processing conditions. First, the self-assembling nature of the TMV coat protein can be altered to produce new geometries, and TMV can also be combined with silica and polymers where TMV plays a templating role for these materials. Second, a number of positioning methods have been developed for TMV. Individual TMV particles have been directly manipulated by AFM,[85] but fabrication techniques to quickly produce patterns of TMV over large surfaces have only recently started to materialize. Some of these techniques, such as convective deposition or stamping, directly manipulate the particles by force while others, such as lift-off and DNA hybridization, control location by chemical processing.

A. Self-assembly

Assemblies of nanoscale rods and disks can be made from modified TMV proteins by controlling the chemistry of

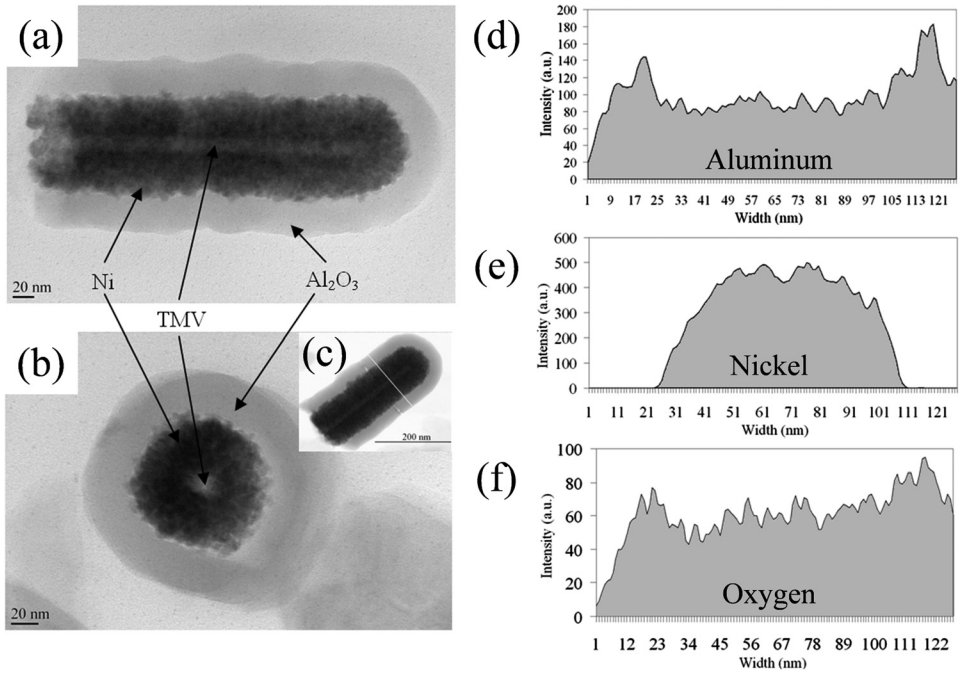

FIG. 9. Side (a) and bottom (b) view TEM images of TMV particles coated with layers of nickel (electroless plating) and Al_2O_3 (ALD)—EDS line-scan data of the STEM image (c) are shown in the (d)–(f) for the elements of interest (Al, Ni, O). Reprinted with permission from K. Gerasopoulos, M. McCarthy, P. Banerjee, X. Fan, J. N. Culver, and R. Ghodssi, Nanotechnology **21**(5), 055304 (2010). Copyright 2007, IOP Publishing.

the assembly environment.[86] Plasmids for the expression of TMV coat protein with an attached histidine group were constructed so it could be produced by bacteria. The hexahistidine (His) tag is an amino acid that attaches to the N- or C-terminus of proteins and is commonly used in purification of recombinant proteins. When this modified version of the TMV coat protein assembles into rods or disks, the His residue is presented on the outer surface of the structure. With the His tag added to TMV coat proteins, they can be controllably organized into fibers, bundles, hexagonal arrays of disks, or vertically stacked disks (Fig. 10). Assembly is controlled by manipulating phosphate buffer concentration, *p*H, and addition of nickel-NTA (nitrilotriacetic acid) complex or ethanol. It is believed that ionic concentration affects the charge screening of the coat protein surface charges and hence assembly interactions on the outer surface of the coat protein. On the other hand, *p*H affects assembly of the coat proteins into their naturally preferred helical structures. The His tag produces attractive interparticle interactions and allows the organization of bundles or arrays; however, addition of Ni-NTA complex to the solution inhibits this effect. By significantly expanding the possibilities of the geometric organization of TMV, more sophisticated mineralization templates are possible.

To produce TMV-templated silica nanostructures,[87] a crystalline birefringent gel was prepared from TMV and then coated with silica by condensation of SiO_2 from the hydrolysis of a TEOS solution. The resulting structure was dried and calcined to remove the TMV. Two possible configurations were observed. One format is a hexagonal organization of 11 nm diameter linear channels with 9–10 nm thick silica walls, arranged with a 20 nm unit cell periodicity. The other format is radiating linear channels (10–15 nm in width) of mineralized TMV fragments around a silica core that form a 100–140 nm spherical particle. This new form of TMV templated silica could be used as a silica metamaterial with applications in optics.

Continuous conductive nanowires of significant length are desirable for electronics applications, but they are

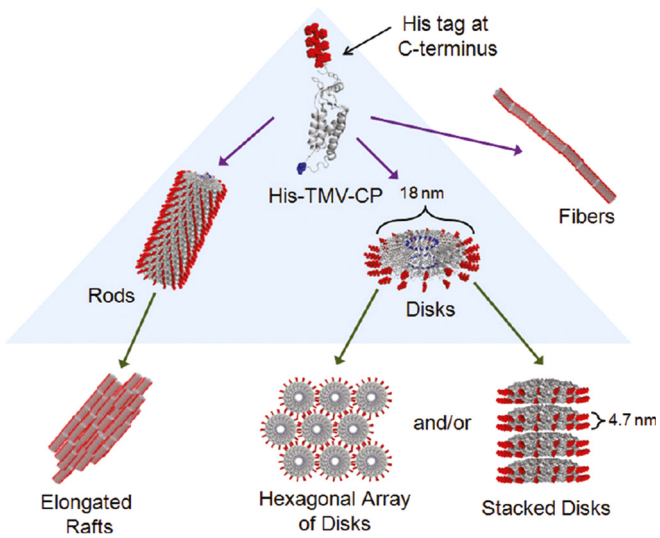

FIG. 10. (Color online) Self-assembling structures of TMV CP (incorporated His tag shown on the outer extremity of each coat protein). Transitions in the highlighted region also occur for wild-type TMV CP. Transitions outside the highlighted area occur for TMV CP over time, with the rate of formation dependent on solution *p*H and ionic strength. Reprinted with permission from M. A. Bruckman, C. M. Soto, H. McDowell, J. L. Liu, B. R. Ratna, K. V. Korpany, O. K. Zahr, and A. S. Blum, ACS Nano **5**(3), 1606 (2011). Copyright 2011, American Chemical Society.

difficult to fabricate in practice. A conductive polymer (polyaniline) has been combined with TMV to produce head-to-tail assembled TMV with a continuous coating[88] in single nanofibers or nanofiber bundles. It was found that the morphology can be controlled by *p*H to produce short fibers, long bundled fibers or long single fibers. At room temperature, the bulk DC conductivity of dried films of TMV/polyaniline fibers was measured by four-point probe and was found to be in the range of 0.01–0.1 S/cm. This is comparable to the polyaniline nanofibers synthesized by other methods. TEM and SAXS studies show that *p*H affects the branching of polyaniline. The branched polyaniline surface makes very long self-assembled nanofibers possible by preventing the lateral association during head-to-tail assembly.

Related work with doped polyaniline and polypyrrole nanowires with lengths of several micrometers was also reported.[89] Polyaniline (PANI) was polymerized on the surface of suspended TMV under various conditions using poly(styrene sulfonate), PSS—a negatively charged dopant for polyaniline that increases electrical conductivity. Short rods, bundles, and single long fibers could be produced by varying the *p*H. The polymerization solution *p*H affects the length of fiber formation, and addition of PSS affects bundling due to surface charge and steric interactions (Fig. 11). Scanning spreading resistance microscopy (SSRM) was used with contact mode AFM and the measured conductivity of the fibers is within expected values for PSS doped PANI. Such *in situ* polymerization processes can be tuned to favor short fibers, long individual fibers or long bundles of fibers. The reported values of conductivity are not as high as semiconducting nanowires (order of 1 S/cm) or carbon nanotubes (1–5 S/cm), but are similar to PANI nanofibers produced by other methods. These composites have potential application in electronics, optics, sensing, and biomedical engineering.

B. Directed positioning and patterning

Individual TMV particles can be aligned by a relatively simple processes involving fluid and air flow.[50] In this method, TMV particles in an aqueous solution are oriented by blow-drying of a droplet or by removing a droplet by capillary forces with filter paper. The viruses are aligned in the direction of fluid flow, most likely due to shear forces near the fluid–surface boundary. The forced air method was suitable for surfaces with strong TMV interaction such as highly polar surfaces, and lateral suction of the liquid was suitable for surfaces with weak TMV interaction, such as carbon. The authors state that the typical diffusion time for a TMV particle in the droplet to the surface is about 1 h for concentrations of 0.1 mg/ml. This demonstrates a straightforward way to form aligned TMV without the need to produce monolayers or liquid crystals.

A detailed study of the process parameters during convective deposition of TMV was conducted and found to produce

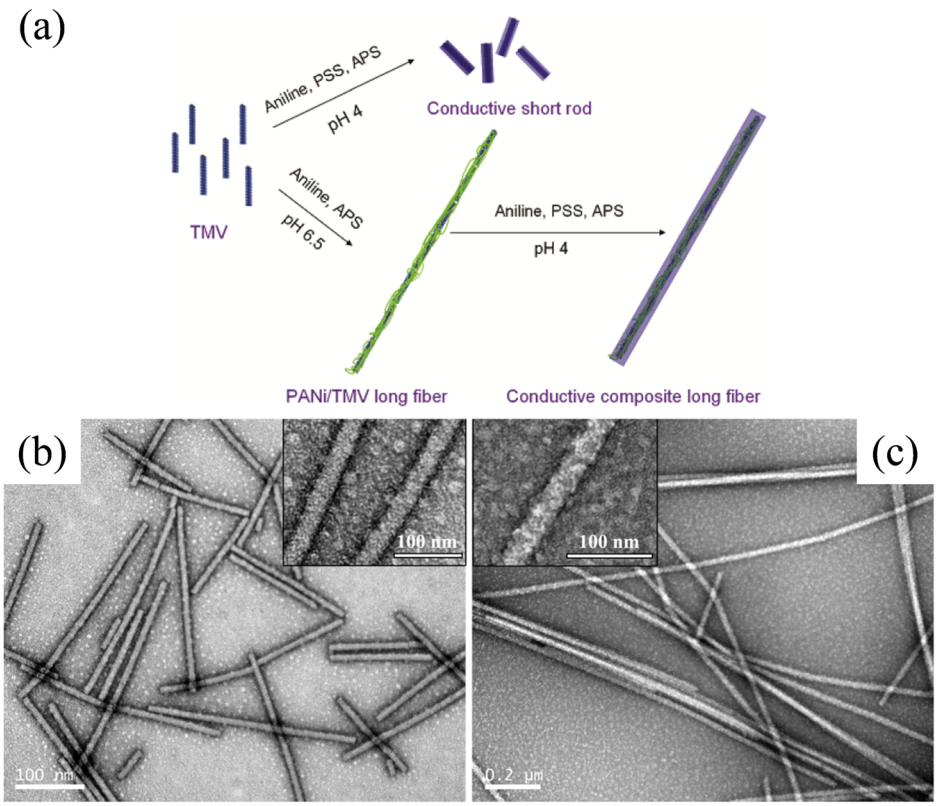

FIG. 11. (Color online) (a) Schematic of the fabrication of conductive polyaniline/TMV composite nanowires. Similar processes can be used to prepare composite nanofibers with other conductive polymers (for example, polypyrrole, Ppy). TEM images of (b) PSS/PPy/TMV composite nanowires, and (c) PSS/PPy/LF composite long fiber using pyrrole as starting materials. Reprinted with permission from Z. Niu, J. Liu, L. A. Lee, M. A. Bruckman, D. Zhao, G. Koley, and Q. Wang, Nano Lett. **7**(12), 3729 (2007). Copyright 2007, American Chemical Society.

TMV in a variety of orientations and thicknesses (Fig. 12).[90] During convective deposition, TMV is deposited from a liquid suspension that is held between a moving glass slide and the substrate. An assembly front forms at the leading edge of the liquid and a drying front follows the trailing edge of the glass slide. The surface roughness of the final TMV film was a function of the surface energy of the substrate, where increasing surface roughness correlates to increasing water contact angle. The orientation, packing density, and thickness vary significantly but controllably with virus concentration and assembly speeds. Four assembly regimes were observed: (1) incomplete monolayer with parallel orientation, (2) monolayer with parallel orientation, (3) multilayer with disordered orientation, and (4) multilayer with antiparallel orientation. TMV is a useful mineralization template, and controllable and well-ordered arrays could be used in nanomanufacturing and production of continuous nanowires.

Nanoscale printed lines have been derived from microscale templates[91] using oxygen plasma treated polydimethylsiloxane (PDMS) stamps. Theses stamps are used to transfer TMV onto oxidized silicon surfaces. The wettability of the aqueous TMV "ink" is adjusted by adding ethanol and using different drying methods. The authors propose that the dewetting process of the ink on the molds affects how the ink is deposited. TMV-based ink can be distributed on the edges of mold's features, enabling nanoscale features from microscale stamps. A related stamping technique uses controlled wrinkling of PDMS to produce stamp features tuned between 130 nm and 1 μm.[92,93] A flat PDMS film is stretched and oxidized in an air plasma. When relaxed, the film forms regularly spaced wrinkles that can be used as a template to organize TMV into continuous lines. Using optimized processing conditions for TMV coating, aligned TMV rods are present in the grooves but not on the ridges, and the patterned TMV could be stamped onto oxidized silicon surfaces. Using a stamp with 300 nm periodicity, ordered arrays of TMV were produced with spacing between 276 and 305 nm. Mineralization of the templated TMV could produce continuous nanowires of several micrometers arranged in a regular array.

By using genetically modified TMV, standard microfabrication processes can be used to pattern TMV instead of techniques specific to the virus and particular surfaces. The research group at the University of Maryland has pioneered the integration of biological self-assembly with top-down microfabrication processes, which greatly enhances the patterning capabilities of genetically modified viruses for device applications. Based on the nickel metallization process of TMV-1Cys,[63] lift-off was demonstrated to be compatible with TMV-1Cys in both Ni-coated and uncoated configurations (Fig. 13).[32] Lift-off is a standard microfabrication technique where a patterned photoresist masked is used to define areas where a layer (typically metal) should be removed at the end of the process. In the case of bare TMV-1Cys, the photoresist is either dissolved in acetone with ultrasonication or a standard photoresist developer was diluted with sodium phosphate buffer to reduce its *p*H. The photoresist mask could be removed since it was flood exposed prior to TMV coating.

TMV-1Cys preferentially aligns in the direction perpendicular to the substrate. The mechanisms of virus assembly in this system are not completely understood, and to the authors' knowledge, a systematic study has not been reported. However, it is known that wild-type TMV does not produce vertically self-assembled rods as TMV-1Cys does. The self-assembly most likely involves a combination of multiple factors: (1) metal–thiol bonding at the 3′ where the

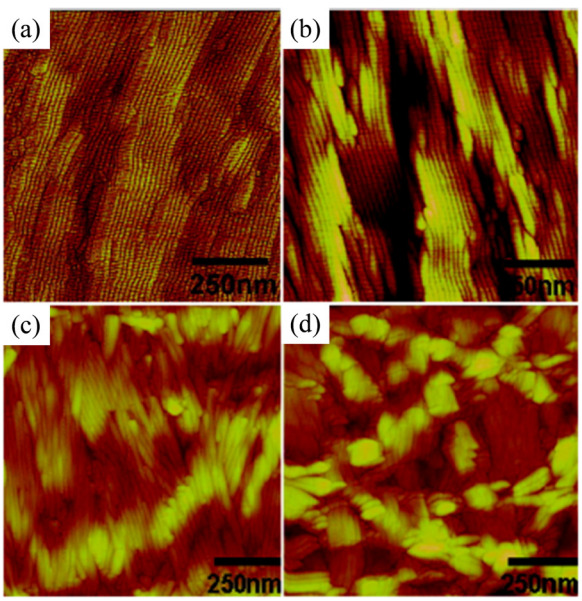

FIG. 12. (Color online) AFM images of TMV assembled onto (a) amine-, (b) silicon oxide-, (c) acryloxy-, and (d) methyl-terminated surfaces. The images reveal a strong dependence of viral ordering on the surface energy of the substrate as seen by the average surface roughness. Reprinted with permission from S. P. Wargacki, B. Pate, and R. A. Vaia, Langmuir **24**(10), 5439 (2008). Copyright 2008, American Chemical Society.

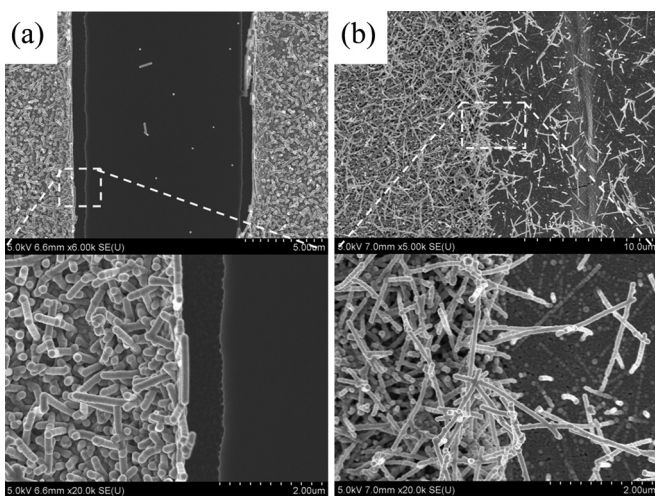

FIG. 13. SEM images of TMV-1Cys that was first patterned using a lift-off technique with (a) 5:1 buffer:developer mixture and (b) acetone. The TMV-1Cys was then coated with nickel to verify postpatterning chemical functionality. Images (c) and (d) show close-up views of the textured surfaces. Reprinted with permission from K. Gerasopoulos, M. McCarthy, P. Banerjee, X. Fan, J. N. Culver, and R. Ghodssi, Nanotechnology **21**(5), 055304 (2010). Copyright 2007, IOP Publishing.

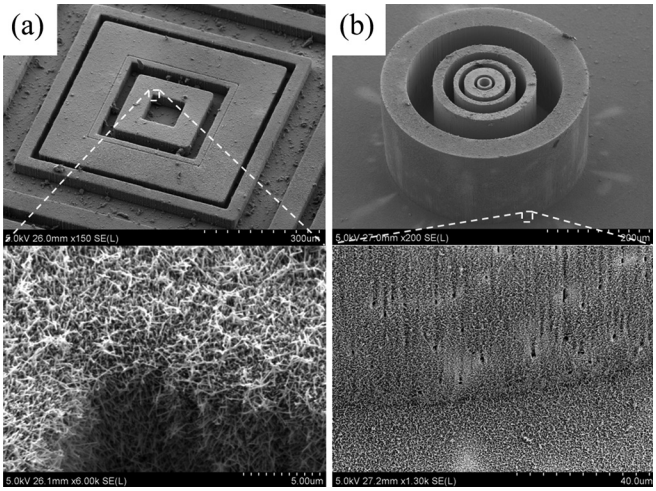

FIG. 14. SEM images of three-dimensional microstructures covered with TMV-1Cys/Ni, (a) SU-8 structures, (b) structures etched in silicon. Bottom pictures (c) and (d) show exploded views of the textured surfaces outlined by the dotted areas in (a) and (b). Reprinted with permission from K. Gerasopoulos, M. McCarthy, P. Banerjee, X. Fan, J. N. Culver, and R. Ghodssi, Nanotechnology **21**(5), 055304 (2010). Copyright 2007, IOP Publishing.

cysteine group is more exposed than other parts of the virus, (2) steric effects at particular solution concentrations, (3) the natural tendency of the virus to self-align side-by-side in solution, (4) the surface roughness of the substrate, and (5) random Brownian motion of the virus in solution at room temperature.[63] After the TMV-1Cys self-assembly, the following metallization creates a conductive high surface area coating in specified areas. The fidelity of the resulting patterns is limited only by the contact photolithography critical dimension (2 μm). TMV-1Cys coatings were also integrated onto silicon and SU-8 three-dimensional microstructures with excellent coverage of both horizontal and vertical surfaces (Fig. 14). The high surface area metal is a result of the preferential vertical alignment of TMV. The orientation is "captured" when coated with nickel which creates a highly mechanically and thermally stable template. Development of TMV-compatible microfabrication processes allows the incorporation of more functional materials with TMV and integration of nanostructures into new devices. Expected applications are high sensitivity sensor arrays, complex micro/nanostructures with textured surfaces, and nanostructured electrodes for energy storage devices.

Finally, the DNA hybridization approach was used for the direct bottom-up assembly of the TMV CP to produce virus-like-particles (VLP) on specific areas of a substrate.[94] Polymer blend lithography was used to prepare the surface of silicon wafers. The exposed silicon areas were chemically functionalized so that linker DNA strands could be attached, and then sequentially exposed to TMV RNA and TMV CP. The linker DNA forms a capture site for TMV RNA in solution, and CP assembly occurs around the RNA strand to produce a VLP derived from the building blocks of TMV. The VLPs form only in areas coated with the DNA linker strand, but the VLPs are flat on the silicon surface and are randomly orientated (Fig. 15). The authors expect that the polymer blend lithography approach combined with bottom up assembly of monomeric building blocks could improve integration of hybrid TMV materials with microdevices.

V. SENSING APPLICATIONS

Tobacco mosaic viruses possess many attractive traits that are highly coveted for sensor applications. TMV is a high-aspect ratio nanostructure that has the potential to express a high binding site density. Their ability to be genetically engineered not only permits them to have a high selectivity toward a single analyte but also enables the design and creation of different constructs for a wide range of analytes of interest. Furthermore, its robustness and tolerance to *p*H and temperature levels allow TMV to be readily integrated as receptor layer within sensor systems. In this section, the use of TMV for chemical and biological sensing and their development toward miniaturized sensor platforms is described. TMV can utilize both of its main physiological components, RNA and coat proteins, as a binding probe for specific recognition of analytes.

A. RNA probe for DNA hybridization

The viral RNA usually provides a backbone structure for the coat proteins self-assembly. This RNA can also be used as a probe for DNA hybridization sensors.[95,96] These sensors

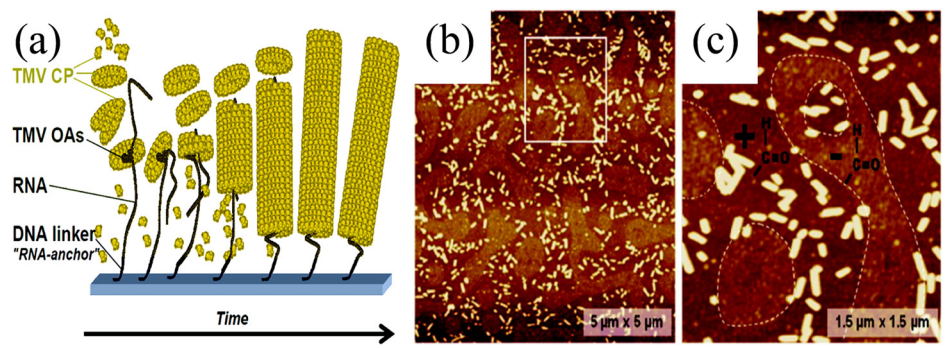

FIG. 15. (Color online) (a) Schematic diagram of RNA-guided bottom-up assembly of TMV CP that are spatially directed to surface patches predefined by polymer blend lithography. (b) AFM topography image of TMV CP rods with site-specific assembly, and close-up is shown in (c). Reprinted with permission from A. Mueller, F. J. Eber, C. Azucena, A. Petershans, A. M. Bittner, H. Gliemann, H. Jeske, and C. Wege, ACS Nano **5**(6), 4512 (2011). Copyright 2011, American Chemical Society.

are investigated and developed with potential applications in genomic sequencing, mutation detection, and gene therapy discovery. Controlled disassembly of coat proteins can expose the 5′-end of TMV-1Cys, allowing for complementary DNA hybridization with the exposed segment of the RNA.

This partial virion disassembly of the viral genome is realized by adjusting the virus solution to *p*H 8. It is then pelleted by centrifugation to remove free coat proteins. Yi *et al.*[34] first demonstrated that TMV can be attached onto patterned surfaces on a microfabricated chip by immobilizing complementary DNA probes. Fluorescent imaging, used to visualize and characterize the assembly of TMV, was made possible by a thiol reactive fluorescent marker on the outer surface of TMV-1Cys. The advantage of labeling TMV over conventional DNA or DNA probes is the high density of fluorescent tags that can be realized on the surface of the TMV, inducing a stronger fluorescent signal per DNA hybridization.

Patterned silicon chips were prepared for the spatially selective assembly of TMV nanotemplates via hybridization containing (1) no DNA oligos, (2) oligos complementary to the TMV 5′-end, and (3) noncomplementary oligos sequence. Figures 16(a) and 16(b) show that only the patterned electrode link to the TMV-specific probe was bounded to the TMV-1Cys templates. Nonspecific binding was not observed on neither the bare electrode nor the noncomplementary oligos. A negative control was conducted to confirm that the exposed RNA at the 5′-end was the sole participant in the hybridization. This study demonstrated the dual ability of TMV-1Cys to act as a selective probe for DNA hybridization and to express a fluorescent indicator for ease of characterization.

Yi showed that the TMV-1Cys RNA probe platform can be further developed into hybridization-based assembly of DNA using the viral nanotemplates.[43] By taking advantage of the partially exposed RNA in the TMV-1Cys nanotemplates, the virus can be prehybridized with a DNA linker. This DNA linker is designed to be complementary to the exposed TMV-1Cys RNA on the first half of the linker. On the remaining half, it is programmed to match a capture DNA probe sequence that is selectively immobilized on a chip surface (Fig. 16). The prehybridized TMV-1Cys can then be self-assembled onto addressable DNA probes. To differentiate between two differently programmed DNA linkers, colored fluorescence (Cyanine dyes, Cy5 and Cy3 maleimide) were labeled onto the surface of TMV-1Cys.

Concentrations of hybridization mixtures varying from 16 to 500 μg/ml were used to show correlated fluorescence intensity. No cross-hybridization between the two programmed TMV-1Cys-DNA-linkers and capture DNA probes was observed. Finally, a negative control was conducted using DNA probes complementary to the 5′- and the 3′-end to show the complete hybridization at the 5′-end with the linker DNAs and that the disassembly process does not result in the unravel at the TMV 3′-end. This platform has demonstrated its ability to specifically address an electrode based on the selectivity of the programmed hybridization sequence, which is useful for selective immobilization of receptor layers for sensor applications.

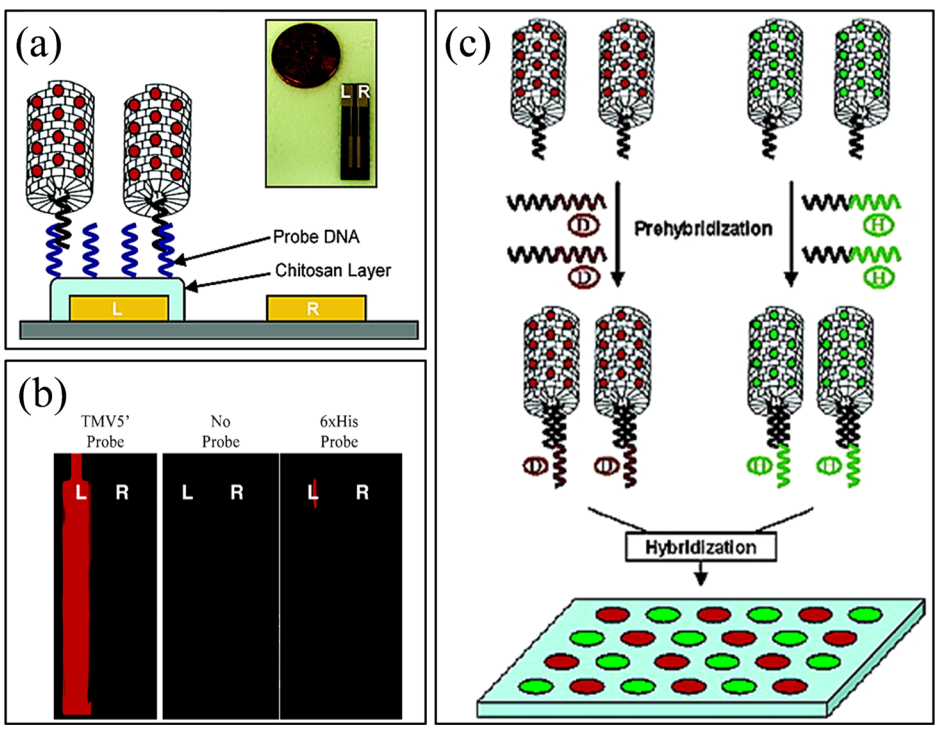

FIG. 16. (Color online) (a) Diagram showing exposed RNA selectively hybridizes with DNA probes immobilized on a chitosan layer compare to a bare gold electrode. (b) Fluorescent imaging showing selective hybridization relative to bare gold electrode as well as no probe and 6xHis Probe. Adapted from Ref. 34. (c) Flow diagram showing hybridization-based programming of two types fluorescently labeled and partially disassembled TMV-1Cys nanotemplates for assembly onto DNA oligonucleotide microarray platform. Adapted from Ref. 43.

To accommodate a larger variety of programmable DNA sequences without introducing additional fluorescent labeling differentiation, a microfabricated barcode identification platform was realized. Tan *et al.*[44] was able to build upon the platform by integrating the fluorescently labeled TMV-1Cys RNA probe within a polyethylene glycol (PEG) microparticle using a previously developed microfluidic system. Each microparticle is spatially divided to consist of (1) an encoded identity information for the type of DNA capture probe, (2) internal control segment, and (3) DNA capture probe of different types. The encoded identity information is an imprinted barcode in Rhodamine grafted PEG monomer using stop-flow lithography. The DNA capture probe is also grafted with PEG monomer on the other half of the PEG microparticle.

It was shown that the fluorescein-labeled TMV-1Cys-DNA-linker was successfully assembled onto microparticles via hybridization. The middle internal control segment, in the absence of DNA capture probe, showed minimal fluorescent display, demonstrating low nonspecific binding and high spatial selectivity. Sequence specific assembly was demonstrated when fluorescent signal was only observed on microparticles with the correct barcode that is linked to the matched complementary capture DNA.

The fluorescent intensity across the microparticle was relatively constant, indicating that the fluorescein labeled TMV-1Cys-DNA-linker was uniformly hybridized onto the surface. The fluorescent intensity of the fluorescein labeled TMV-1Cys was compared with that of single-stranded DNA (ssDNA) using confocal microscopy. The fluorescent signal from TMV-1Cys was visually more intense compared to that of ssDNA, due to high fluorescein molecule density expressed on the nanostructure. This work demonstrates the TMV's ability to be fully integrated with microfabricated structures in a microsystem environment.

B. Detection using coat protein modifications

The RNA of TMV provides a single selective binding site for DNA hybridization, but the outer surface of the TMV coat protein possesses thousands of sites that can be used for selective binding as well. In addition to the many combinations of amino acids already expressed in the wild-type TMV coat protein, additional custom sequences can be attached to either the C- or N-terminus of the coat protein. For example, we have highlighted the functionality of TMV-1Cys and TMV-2Cys to target thiolated binding. One process that takes advantages of the conjugated cysteine is the electroless deposition of palladium, described in Sec. III. With careful process control, palladium nanoparticles can be nucleated on each cysteine conjugation. Srinivasan[97] took advantage of this platform and conducted hydrogen sensing utilizing palladium coated TMV-1Cys on a microfabricated surface acoustic wave (SAW) transducer. A frequency response was observed for 0.2–2.5% hydrogen stimulation, showing reversible adsorption and desorption.

Bruckman *et al.*[45] chemically functionalized wild-type TMV with oligoaniline (TMV:OANI) for volatile organic compounds (VOCs) sensing. An impedance was taken across two electrodes, measuring the change in conductance through the TMV:OANI receptor layer. Experiments show that TMV:OANI has great selectivity toward ethanol and methanol over other VOCs tested. The authors suggested that the selectivity of TMV:OANI over wild-type TMV is due to the flexoelectric properties of wild-type TMV.[98]

The coat protein has also been shown to display a wide range of conjugations on its outer surface, including specific sequences of oligopeptide. Short sequences of peptides are especially interesting due to their potential for extremely high affinity to a selective target. Recent approaches have utilized phage display to study and screen the bond strength between libraries of short peptides (typically 8–12 amino acids long) and the analyte of interest.[99,100] To date, this method has been employed to identify numerous single chain antibodies as well as receptor peptides that bind various pathogens and toxins of importance to food safety, including shiga toxin, staphylococcal enterotoxin B and *Escherichia coli* O157:H7.[101–106] Many of these receptor peptides display binding affinities in the nanomolar range and are capable of detecting their target molecules in traditional ELISA systems at the nanogram level.[107,108] Flexibility and integration are two important factors in the development of a robust but yet versatile sensing system. The robustness of the architecture and genetic tunability of TMV make it a uniquely flexible platform for the controlled display of peptide receptors on various substrates.

The parameters needed for the optimal assembly and patterning of virus-particle containing configured receptor peptides onto active microsensor surfaces have been studied. As a proof of concept, a genetically modified TMV was created to express a trinitrotoluene (TNT) receptor peptide on the N-terminus of the coat protein.[41] The modified viruses (TMV-TNT) were self-assembled onto the gold electrode surface of a quartz crystal microbalance (QCM) and exposed to TNT vapor. This sensor tracked changes in resonant frequency as an indication of changing mass due to TNT binding. Results showed enhanced TNT affinities of approximately 300% and 50% for TMV-TNT surfaces as compared to uncoated and TMV-1Cys only coated control transducer surfaces, respectively. This was the first demonstration of selective sensing utilizing a virus based receptor layer for TNT detection. Genetically programmable viruses can be used as a means to display and integrate receptor peptides within transducer systems.

TMV-TNT has also been used as a binding agent in an electrochemical sensor for TNT sensing that is more easily miniaturized compared to a QCM. TNT has an electrochemical signature of three distinctive peaks, due to the reduction of its three nitro groups. The peak current shows linear dependency on TNT concentrations in the system. By introducing TMV-TNT to the TNT solution, a lower reduction current was observed (Fig. 17). This is due to TNT binding to the added peptide, causing the loss in mobility of TNT molecules which results in lower reduction currents.[109] The difference in peak current between utilizing unmodified TMV and TMV-TNT grew to a saturated difference of 4.5 μA starting at 4.3 μg/ml TNT concentration (46% of the

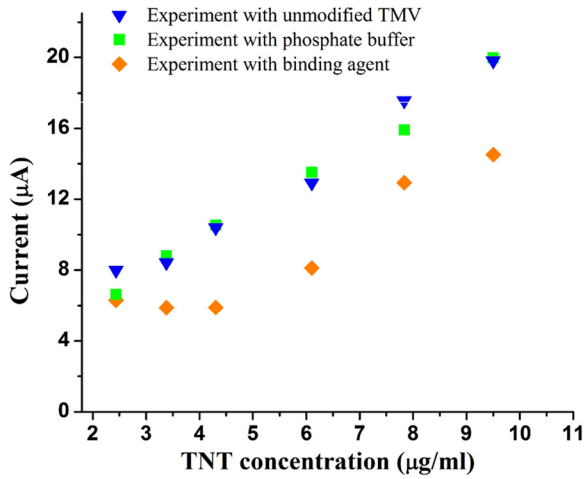

FIG. 17. (Color online) Peak currents of TNT reduction using phosphate buffer, unmodified TMV and TMV-TNT-BP binding agent.

absolute peak current compared with control). This current difference can be used for selective TNT sensing for TNT concentration below 4.3 μg/ml.

VI. ENERGY STORAGE APPLICATIONS

Nanostructured electrodes exhibit several advantages for applications in battery electrodes. First, they demonstrate higher electrode/electrolyte contact area leading to faster ion intercalation/extraction kinetics. Second, nanostructuring shortens diffusion lengths for both electrons and ions, enabling the use of materials with lower conductivities. In addition, nanostructured materials can better accommodate strain generated by ion insertion/removal in systems based on intercalation chemistry, which improves the cycle life of the battery.[110] The microbattery is a special class of energy storage devices, which provides autonomous power for microdevices and microsystems. Such miniaturized systems usually require the energy storage device to be embedded in a small area on a chip. This makes the energy and power density per footprint area a key consideration for small-scale power applications.[111,112] Nickel-coated self-assembled TMV nanoforests[63] show almost an order of magnitude increase in surface area compared to planar substrates. In addition, 3D porous nanonetworks formed by densely packed TMV particles provide space for the volume expansion of materials caused by ions intercalation, which is especially important for alloying anodes.[113,114] In this section, we discuss the fabrication and electrochemical performance of TMV-1Cys-templated electrodes for nickel–zinc and lithium–ion batteries.

A. Nickel–zinc batteries

Nanostructured TMV-1Cys-templated nickel, prepared using ELD, has been tested as a cathode in Ni-Zn batteries.[36] The electrochemical experiments were carried out in potassium hydroxide electrolyte with a zinc strip used as an anode. Planar nickel electrodes were used as a reference to evaluate electrochemical performance of TMV-1Cys-templated nickel electrodes. The latter consistently outperformed flat electrodes and showed stable twofold increase in capacity after 15 cycles, which was attributed to the high surface area of the virus-templated electrodes.[63]

Integration of TMV self-assembly and nickel coating into standard MEMS fabrication process was demonstrated for the first time in a nickel–zinc microbattery with microfluidic packaging scheme (Fig. 18). Devices with and without TMV structures were fabricated and their electrochemical performance was characterized. The initial capacity of microbatteries utilizing viral nanostructures demonstrated a sixfold increase compared to cells without virus.[36] These results, combined with robustness of TMV self-assembly and metallization, demonstrated feasibility of developed technology to be used in higher performance energy storage devices.

B. Lithium–ion batteries

Rechargeable lithium–ion batteries provide the highest energy density combined with reasonably good power

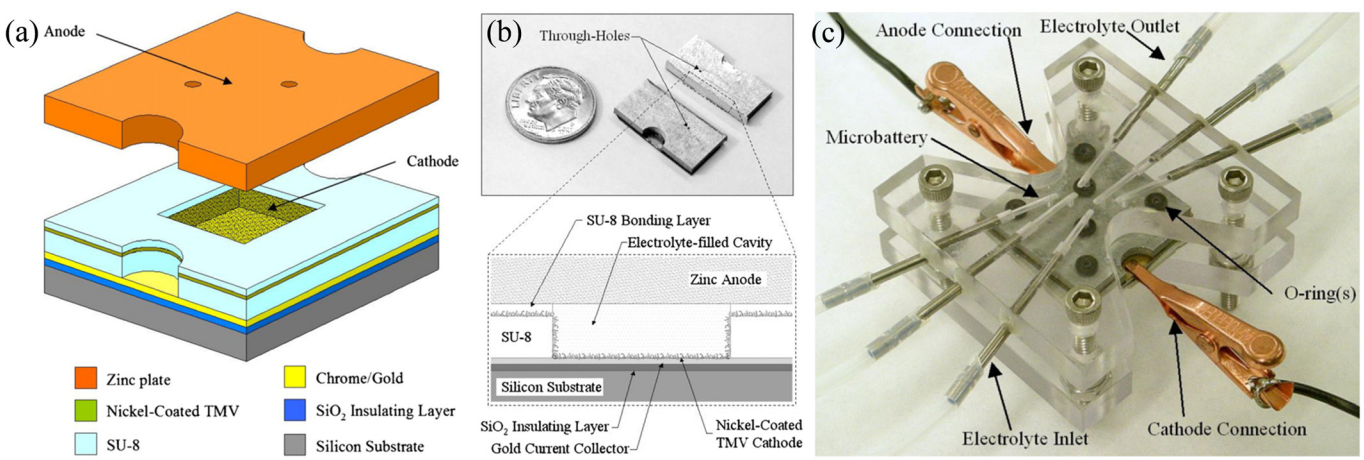

FIG. 18. (Color online) Ni-Zn microbattery with nanostructured TMV-1Cys-templated electrodes: (a) Schematic of microbattery layers, (b) Photograph of the device diced in half and its cross-sectional schematic; (c) Photograph of a packaged microbattery showing the fluidic and electrical connections. Reprinted with permission from K. Gerasopoulos, M. McCarthy, E. Royston, J. N. Culver, and R. Ghodssi, J. Micromech. Microeng. **18**(10), 104003 (2008). Copyright 2007, IOP Publishing.

efficiency among all energy storage systems.[115,116] Fabrication of lithium–ion battery electrodes using TMV involves an additional step for the deposition of active material on high surface area virus-structured nickel current collectors. This is usually implemented by combining a nickel plating process with conformal thin-film deposition techniques such as ALD, electrodeposition or sputtering.[32,35,76–80,117] This method produces core/shell nanocomposite electrodes with a conductive nickel core and active battery material forming the outer layer. Direct contact between current collector and every position of lithium intercalating film enables very fast charge transport for electrons and ions, essential for enhanced battery performance.

TMV-1Cys-templated silicon electrodes were fabricated using physical vapor deposition of undoped[77] and n-type[76] silicon as well as silicon electrodeposition.[76] Silicon belongs to a family of active lithium–ion battery materials, referred to as alloying anodes.[113,114] These materials generally suffer from a poor cycling behavior due to the large materials volume change during lithium cycling. The excellent cycling stability of virus-templated silicon electrodes was attributed to the unique 3D porous architecture formed by TMV template. After silicon expansion, caused by lithium intercalation, the silicon coating remained in contact with the conductive nickel core. Further cycling resulted in formation of a sponge-like silicon structure [Figs. 19(c) and 19(d)]. Resistance to the stress associated with silicon expansion was attributed to the mechanical integrity between silicon and nickel. In addition, charge transfer resistance was significantly reduced for highly conductive n-type silicon, as indicated by electrochemical impedance spectroscopy.[76] Similar results were obtained for the TMV-1Cys-templated tin anode, prepared by pulse electrodeposition of tin onto nickel-coated self-assembled TMV structures.[78] Therefore, availability of space in the porous electrode for active material volume increase combined with the mechanical integrity of TMV-1Cys/Ni/Si or TMV-1Cys/Ni/Sn surfaces likely accounts for observed enhanced electrochemical behavior.

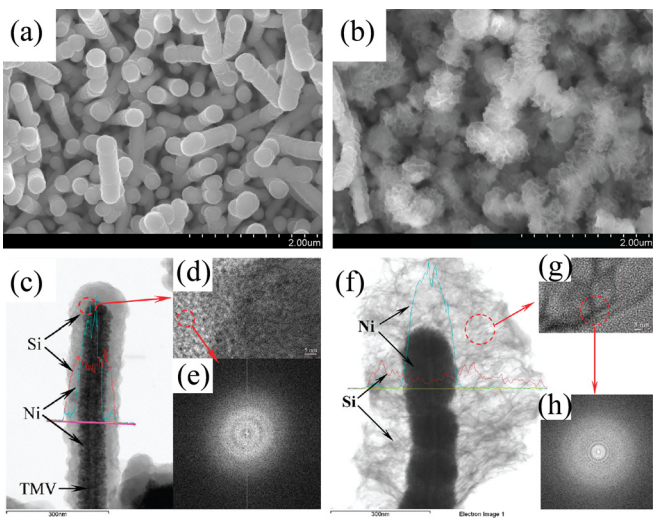

FIG. 19. (Color online) SEM images of (a) pristine TMV-1Cys-templated Si electrode and (b) after 75 cycles at 1 C. (c) TEM image of a pristine single TMV-1Cys-templated particle with EDS profiles of Ni and Si with corresponding (d) HRTEM image and (e) FFT image of silicon layer. (f) TEM image with EDS spectra for nickel and silicon after 75 cycles at 1 C with corresponding (g) HRTEM image and (h) FFT image of silicon layer. Reprinted with permission from X. Chen, K. Gerasopoulos, J. Guo, A. Brown, C. Wang, R. Ghodssi, and J. N. Culver, ACS Nano **4**(9), 5366 (2010). Copyright 2010, American Chemical Society.

Atomic layer deposition has proven itself as the most appropriate method for TMV-1Cys-templated materials synthesis due to its ability to produce conformal coatings on complex three-dimensional architectures.[74] Applicability of ALD for the fabrication of both lithium–ion battery anodes and cathodes was demonstrated by depositing TiO_2 (anode) and V_2O_5 (cathode) on nickel-coated virus-templated nanoforests.[35,80] ALD produced thin nanolayers of active battery materials thus maintaining high surface area of the electrodes established by self-assembled TMV-1Cys templates [Fig. 20(a)]. The thickness of deposited active electrode materials was ca. 20–40 nm, indicating the high degree of control ensured by the ALD process. The cross-section TEM image [Fig. 20(b)] demonstrates a layered structure for a single virus-templated particle. Moreover, uniform coating achieved by ALD allowed for making electrodes without binders or other additives. Electrochemical cycling of high surface area TMV-1Cys-templated TiO_2 electrodes[35] revealed excellent cycling stability with capacity fading of only 0.024% per cycle. Cycle life tests performed at different current rates for electrodes with and without TMV indicated that the TMV-structured samples notably outperformed planar films.[35] The virus-structured cathode for lithium–ion microbatteries (Fig. 20) was fabricated using ALD V_2O_5 process with ozone as an oxidant.[80] This process produces well crystallized V_2O_5 films without post-ALD annealing which is advantageous compared to the traditionally used H_2O-based V_2O_5 ALD that produces amorphous films, since crystalline vanadium oxide films demonstrate better cycle life.[117,118] The footprint area normalized capacity of the TMV-1Cys-templated V_2O_5 electrodes is consistently eight times higher than that of the planar electrodes at various current rates. At the same time, the capacity retention is similar for both types of electrodes indicating similarly rapid kinetics.[80]

Three-dimensional microelectrodes have been extensively researched as components for next-generation microbatteries.[111,112] Three-dimensional microstructures can increase material loading, and thus energy density, for the same

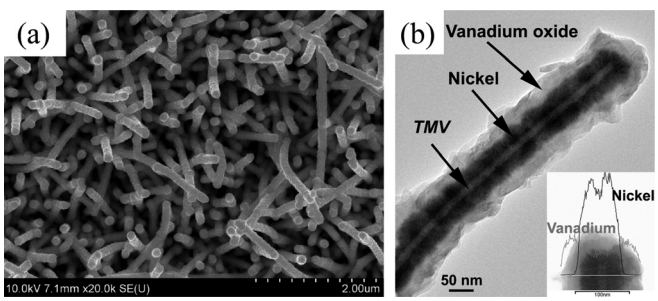

FIG. 20. TMV-1Cys-templated V_2O_5 cathode: (a) SEM image; (b) cross-section TEM image with EDS analysis (inset). Reprinted with permission from E. Pomerantseva, K. Gerasopoulos, X. Chen, G. Rubloff, and R. Ghodssi, J. Power Sources **206**, 282 (2012). Copyright 2012, Elsevier.

device footprint, but lack in power density due to the sluggish diffusion of charged particles. Nanostructures enable faster reaction kinetics, but integration of nanostructured materials into microdevices remains a challenge. Fabrication of hierarchical micro/nanoelectrodes was implemented by following a novel approach that integrated bottom-up TMV-1Cys self-assembly and top-down micromachining processes.[79] In these electrodes, high energy density is achieved due to the active surface area increase (larger material loading) within a given footprint by combining TMV-1Cys with three-dimensional microfabrication processes. The TMV nanostructures enable high power density through larger electrode/electrolyte contact area and faster charge transport due to shorter diffusion lengths.

The unique ability of TMV to be integrated with 3D fabrication techniques pioneered the utilization of hierarchical architectures for microbattery applications.[79] The hierarchical micro/nanoelectrodes were fabricated on silicon wafers with an evaporated gold seed layer. An array of gold micropillars, 60 μm tall and 20 μm in diameter, were electrodeposited in a photoresist mold. The micropillars were coated with the self-assembled TMV-1Cys template followed by electroless nickel plating and deposition of 30 nm thick V_2O_5 using an ozone-based ALD process [Figs. 21(a) and 21(b)]. The reference electrodes without micropillars, referred to as the "electrodes with nanostructures only" were made using similar processes.

Electrochemical cycling indicates that the capacity of hierarchical electrodes at different current rates is consistently three times higher than the capacity of the electrodes with nanostructures only, in agreement with the increase of the surface area added by gold micropillars [Fig. 21(c)]. At the same time, capacity retention, which shows how rapidly lithium ions and electrons transfer, is similar for both types

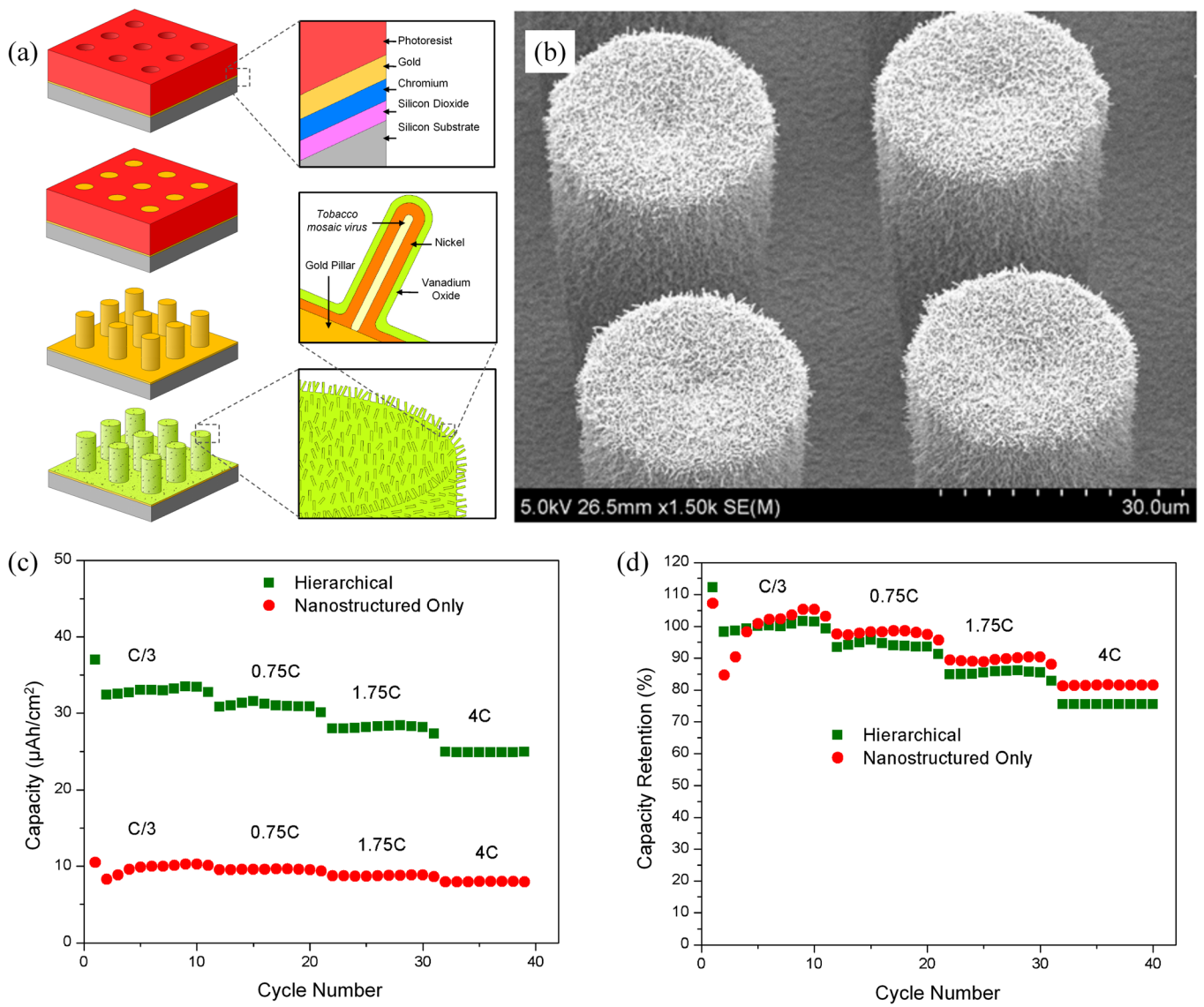

FIG. 21. (Color online) (a) Schematic representation of the hierarchical electrode fabrication. (b) SEM image of hierarchical electrodes. (c, d) Discharge capacity and capacity retention of the cells with the hierarchical electrodes and electrodes with nanostructures only in the voltage range of 2.6–3.6 V (C-rates are indicated in the figure). Reprinted with permission from K. Gerasopoulos, E. Pomerantseva, M. McCarthy, A. Brown, C. Wang, J. N. Culver, and R. Ghodssi, ACS Nano **6**(7), 6422 (2012). Copyright 2012, American Chemical Society.

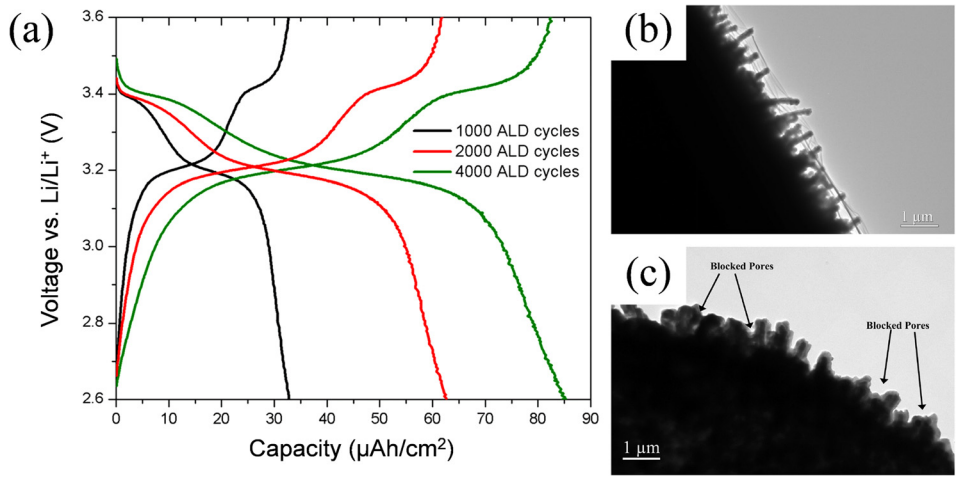

FIG. 22. (Color online) (a) Discharge/charge curves for hierarchical electrodes with different active material thickness at a current of 12 μA; V_2O_5 was deposited for 1000, 2000, and 4000 ALD cycles, aiming at thickness of 30, 60, and 120 nm, respectively. (b, c) Cross-section TEM images taken from the sidewalls of micropillars for samples with (b) 2000 and (c) 4000 ALD cycles of V_2O_5. Reprinted with permission from K. Gerasopoulos, E. Pomerantseva, M. McCarthy, A. Brown, C. Wang, J. N. Culver, and R. Ghodssi, ACS Nano 120606181550007 (2012). Copyright 2012, American Chemical Society.

of electrodes [Fig. 21(d)]. This result indicates that energy density is increased for the hierarchical electrodes without affecting the high rate performance. Further increase in energy density was achieved by increasing V_2O_5 loading (thickness of V_2O_5 film, Fig. 22). When the thickness of V_2O_5 was changed from 30 to 60 nm, the mass loading and capacity changed in linear proportion. However when V_2O_5 thickness was changed from 60 to 120 nm, the capacity increase exhibited a nonlinearity, which was closely related to the increase in mass loading. Cross-section TEM images revealed that the nonlinearity effect was attributed to progressive blocking of open spaces between closely packed adjacent TMV nanorods with increasing thickness of active material [Figs. 22(b) and 22(c)]. These results highlight the importance of controlling both energy and power density of hierarchical electrodes and identify that the optimal thickness of active battery material is close to 120 nm.[79]

VII. DEVICE APPLICATIONS

A great variety of techniques related to TMV-based materials has been described, but the integration of nanomaterials has often been the barrier to broad use of their enhanced properties. In this section, the electronic properties of TMV and its demonstrated capabilities in electronic applications are described. This is followed by the developments of TMV processing to enable integration in bioengineering applications. For each highlighted research work, the TMV-based structures and resulting properties are first described. Second, an explanation of the observed properties is followed by the impact of the methods and their application.

A. Electronics

Piezoresponse force microscopy (PFM) is a technique similar to AFM, where a force is applied and voltage at the tip is measured. The combination of force and voltage provides data about the electromechanical coupling of the material and can be used to calculate piezoelectric and flexoelectric coefficients. Piezoelectric and flexoelectric measurements using PFM were conducted on TMV.[98] The reported value of the piezoelectric response (PRp) is 0.13 pm/V and the flexoelectric response (PRf) is 12 pm/V. However, the calculation of the PRp and PRf involved models with parameters that were not known precisely and were estimated from similar biomaterials. Due to their molecular structure, many biological molecules possess some degree of electromechanical coupling. This technique may produce detailed imaging of biological surfaces (Fig. 23) since piezoresponse topography achieves greater resolution than surface topography alone (at least when the AFM tip is in direct contact with the sample).

The current–voltage (I–V) measurement of TMV coated with platinum nanoparticles has revealed conductivity hysteresis based on applied voltage. The platinum coated TMV can be used like a memristor; however, its behavior does not follow that of accepted memristor models.[119] An aqueous

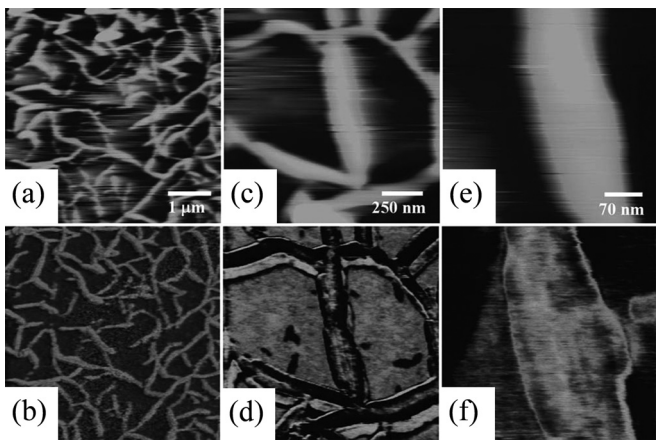

FIG. 23. Surface topography (a), (c), and (e); and piezoresponse images (b), (d), and (f) of TMV at different resolutions obtained by PFM. Reprinted with permission from S. V. Kalinin, S. Jesse, W. Liu, and A. A. Balandin, Appl. Phys. Lett. **88**, 153901 (2006). Copyright 2006, American Institute of Physics.

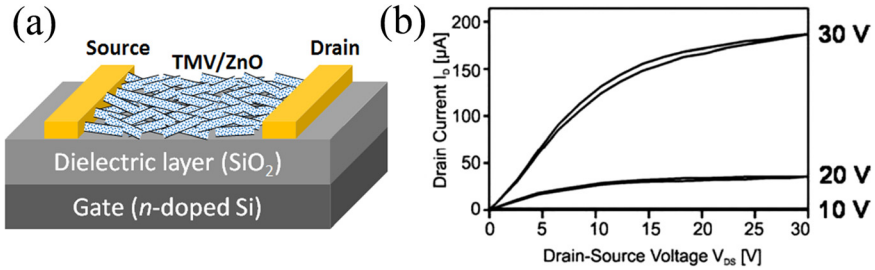

FIG. 24. (Color online) (a) Schematic diagram of the TMV/ZnO FET, and (b) output characteristics of TMV/ZnO for VDS of 0–30 V with VGS from 0–30 V. Adapted from Ref. 68.

solution of the platinum coated TMV was prepared with polyvinyl alcohol (PVA) and then spin coated on a glass substrate with aluminum electrodes. Current–voltage, data cycle, and retention characteristics were measured with a semiconductor parameter analyzer and the results show on-state/off-state switching behavior that can be used for a memory storage device. The memory-like behavior is explained by charge trapping on the nanoparticles, and the electronic conductance by electron tunneling. A similar effect was observed by the same research group for conductive polymers and metal nanoparticles. The semiconductor-like behavior is postulated to arise from an energy barrier at the surface of the coat protein which can be overcome by an external electric field. Charge can be transferred to the platinum nanoparticles from the inner RNA strand where guanine is expected to be a charge donor. Since the PVA matrix and coat protein are insulators, the charge remains on the platinum nanoparticles. This work demonstrated a new kind of nanostructured electronically erasable nonvolatile random-access memory based on an organic/inorganic hybrid.

A related measurement of the resistivity of individual platinum-coated TMV nanorods was conducted by four-point probe.[55] Inspection was performed by SEM, and four-point resistivity measurements of individual TMV/Pt wires made in ultra-high vacuum. The four-point probe measurements of two TMV/Pt nanorods with continuous coatings were 235 $\mu\Omega$ cm and 129 $\mu\Omega$ cm. These measurements are approximately 10 times larger than bulk platinum at 10.5 $\mu\Omega$ cm, but the nanorods were capable of high current densities of 10^5–10^8 A/cm^2. TEM and electron diffraction patterns show a polycrystalline FCC platinum structure. The authors speculate that the high polycrystalinity of the deposited platinum and the possibility of nanoscale gaps in the coating could result in higher measured resistivity of the TMV/Pt nanorod. This measurement of continuously coated TMV/Pt complements the noncontinuous nanoparticle TMV/Pt electrical behavior.[119]

Zinc oxide is an attractive semiconductor material due to high electron mobility, high thermal conductivity, and direct band gap,[120] but it is difficult to use as a semiconductor since control of n-type/p-type conductivity is very challenging. It is interesting to note that TMV coated with ZnO has been evaluated as a FET using I–V characterization, and superior properties were observed compared to thin films by other methods.[68] Multiple ZnO coated TMV particles bridge the gap (in a mat-like sheet) between the electrodes (source and drain) and the n-type silicon substrate beneath a surface oxide layer forms the FET gate (Fig. 24). Control samples were prepared on carboxylate terminated self-assembled monolayer (SAM) coatings and DNA in place of TMV. High resolution TEM shows that the morphology is densely packed ZnO nanoparticles on the TMV surface. Measurements of FET performance were made under argon atmosphere with a semiconductor parameter analyzer. The obtained values for effective charge carrier mobility are summarized in Table II.

The significantly lowered threshold voltage of the TMV/ZnO transistor behavior indicates an electron injection capability of the TMV templates. This is in agreement with STM investigations suggesting that electron transfer across the coat protein is possible, and in agreement with a description of charge trapping in TMV/Pt.[119] The reported charge carrier mobility is favorable compared to other solution-based ZnO deposition methods, and the $I_{on/off}$ ratio is similar to the best reported values. The significantly decreased threshold voltage makes the ZnO based FET much more practically applicable. Furthermore, the process described requires no postdeposition treatments.

Finally, a TMV-templated cupric oxide (CuO) photoelectrochemical (PEC) cell has been developed with the highest photocurrent density reported for nano-CuO.[121] A PEC cell is similar to a solar cell in that it contains a material that absorbs light and generates electricity, but a PEC cell immediately uses it to electrolyze water into hydrogen and oxygen gas. The photoactive material in this PEC cell is CuO sputtered on top of TMV-1Cys/Ni coated with indium tin oxide that forms the current collector. The TMV-templated CuO photocathode possesses a number of advantages that increase the total current photocurrent density. First, the film consists of closely separated nanorods which result in a low charge carrier recombination rate. Second, the nanostructured surface is antireflective since the periodicity of the TMV is smaller than the wavelength of incident light. Third, similar to TMV-templated energy storage electrodes, the charge

TABLE II. FET performance parameters for TMV/ZnO.

ZnO template	Mobility (cm^2/V s)	$I_{on/off}$ ratio	Threshold voltage (V)
TMV (12 cycles)	1.58×10^{-3}	21 000	+2.6
TMV (15 cycles)	1.15×10^{-2}	58 700	+2.1
SAM	1.18×10^{-4}	Not reported	+19.2
DNA	5.52×10^{-5}	Not reported	+9.1

carrier transport distance from the active material to the current collector is short. The result is high photocurrent density, and the geometry could be optimized varying the virus concentration and the sputtering time which affected nanorod spacing and CuO thickness, respectively.

B. Biological and chemical systems

With the aim of producing a material that could be used in bioreactors, nanostructured titania (TiO_2) was formed on TMV templates.[122] First, a silicon wafer is prepared with TMV particles adsorbed onto the surface, and a thin TiO_2 coating is deposited by a sol–gel process. Organic material is then removed by oxygen plasma to produce a TiO_2 shell in the shape of TMV particles. TEM images before and after oxygen plasma show a several nanometer thick TiO_2 coating. The TMV is stable during the coating process; therefore, it is expected that the TiO_2 template is conformal down to the dimensions of individual proteins. Although not demonstrated for TMV, the TiO_2 template could be used as a mold for other materials, allowing them to inherit the precise morphology of TMV. The same templating process was also demonstrated for latex microparticles.

In related work, a microfluidic flow-focusing device produced droplets of PEG hydrogel in a stream of mineral oil that were solidified by photopolymerization under UV light.[123] Two types of TMV (palladium decorated TMV-1Cys or fluorescin labeled TMV-1Cys) can be incorporated into the PEG solution before polymerization, as well as magnetite nanoparticles. Multiple PEG fluid streams can be combined immediately upstream of the flow focusing, producing particles with two halves of different functionality—Janus particles (Fig. 25). Microparticles with magnetic nanoparticles could be moved with a magnetic field, and microparticles with palladium nanoclusters showed catalytic activity as measured by dichromate reduction. The packaging of nanomaterials into a usable and stable macroscale format is a challenge. By incorporating functionalized viral nanoparticles into hydrogel, they can be encapsulated without aggregation and retain their activity.

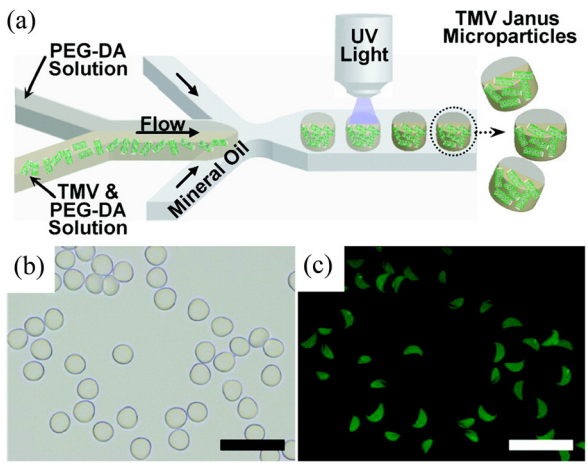

FIG. 25. (Color online) (a) Schematic of producing Janus microparticles, (b) fluorescently labeled TMV Janus microparticles, and (c) Janus microparticles that contain magnetic and catalytic nanoparticles. Reprinted with permission from C. L. Lewis, Y. Lin, C. Yang, A. K. Manocchi, K. P. Yuet, P. S. Doyle, and H. Yi, Langmuir **26**(16), 13436 (2010). Copyright 2010, American Chemical Society.

High surface area TMV-1Cys nanotemplates stabilized on gold surfaces are attractive for heterogeneous catalysis applications. Catalytic activity of TMV-templated nanostructured Pd was studied in the dichromate reduction[46,124] and Suzuki coupling[125] reactions. TMV-1Cys/Pd catalyst chips were prepared by immersing clean gold-coated chips in TMV-1Cys suspension for surface assembly. This was followed by electroless palladium plating that produced Pd nanoparticles (ca. 13 nm) along the virions. Precisely spaced thiol groups on the outer TMV-1Cys surface enabled uniform metal nanoparticle growth and controllable particle size distribution, which are important parameters for heterogeneous catalysis. In addition, the surface-assembled chip-based approach allowed for straightforward catalyst and product separation as well as catalyst recycling. TMV-1Cys/Pd nanoparticles showed good stability in consecutive catalytic cycles,[46,125] unlike many heterogeneous catalysts that are rapidly deactivated under operating conditions. The loading and catalytic activity of Pd nanocatalysts were controlled by the tunable and selective surface assembly since TMV-1Cys preferentially assembles on gold versus silicon nitride and the TMV suspension concentration affects nanoparticle coverage.[124] The facile route utilizing TMV nanotemplates can be extended to the fabrication of new surface-assembled heterogeneous catalysts with tunable loading and precise area-based spatial control.

In contrast to TMV assembly methods that produce positive templates, a method using poly(allylamine hydrochloride) (PAA) uses TMV to produce negative templated materials that exhibit selective absorption of the original TMV shape.[126] To produce the shape-selective PAA, TMV is dispersed into a PAA solution which is subsequently polymerized. The TMV is removed to produce an imprint of the virus in the polymer. The imprinted hydrogel showed selective affinity for *Tobacco mosaic virus* (rod like particles 18 nm by 300 nm) over *Tobacco necrosis virus* (isometric particles about 26 nm diameter), and this material could be used to produce a virus-specific filtering system.

TMV is generally not miscible in nonpolar solvents; however, a chemically modified TMV with poly(ethylene glycol) (PEG) side-chains is soluble in a variety of solvents and possesses increased temperature stability.[127] A two-step chemical treatment involving a diazonium salt and poly(ethylene glycol) alkoxyamine produces TMV coated by PEG chains. The PEG-TMV is selectively precipitated from solution by addition of ammonium sulfate, and the precipitate is redissolved in chloroform where it can be stored. The TMV-PEG was stable at much higher temperatures than normal TMV (up to 160 °C), which was verified by dynamic light scattering measurements before and after heating. TEM verified the integrity of TMV rod after heating in solvents. The PEG side chains enable solubility in hydrophobic liquids, and hydrophobic environments have been demonstrated to increase the stability of proteins. Since the protein structure is stabilized by hydrogen bonds and the hydrophobic solvent does not

have hydrogen bond donors or acceptors, there are no kinetically available intermediate states during protein unfolding at elevated temperatures. It is expected that research will lead to easier integration of TMV into composite materials, such as a polystyrene-TMV composite created as proof-of-concept. TMV-PEG would be more compatible with nanofabrication techniques with a higher thermal budget.

Chemical and genetic modification of TMV has proven to be beneficial for tissue engineering as well. TMV was combined with the peptide sequence GRGDSPG (Gly-Arg-Gly-Asp-Ser-Pro-Gly), referred to as RGD ligand, and mixed with PVA to produce composite electrospun fibers to be used as a cell culture scaffold.[128] TMV was genetically engineered to include the RGD ligand (TMV-RGD) since it can bind to cell surface integrin proteins and promote cell adhesion. TMV mixed with PVA was used to produce a mat of electrospun fibers 300–400 nm in diameter. PVA is biocompatible and TMV is a harmless plant virus. Baby hamster kidney (BHK) cells were cultured on the electrospun fiber mat and monitored by optical microscopy and fluorescent staining of actin. TMV-RGD/PVA nanofiber mats show threefold increase in BHK cell density compared to PVA or TMV/PVA nanofibers.

TMV has been used to produce supramolecular high-relaxivity MRI contrast agents. The TMV was coated with chelated paramagnetic gadolinium(III) ions, and the interior channel or exterior surface of the TMV could be targeted by using chemistries that selectively reacted with tyrosine (exterior) or glutamic acid (interior).[129] The innerchannel coated TMV could be transformed into spherical nanoparticles (SNP) by stabilization with PEG and thermal treatment. The TMV-based gadolinium SNPs had excellent MRI contrast enhancement properties, and the authors suggest that a combination of factors leads to this result. First, the TMV rod is a rigid structure with numerous binding sites for Gd. Second, both the covalent bonding of the Gd to the viral scaffold and the rigidity of the TMV/SNP may explain the enhanced performance as an MRI contrast agent.

It is well known that naturally occurring superhydrophobic surfaces, such as those found on aquatic plant leaves like the lotus, contain hierarchical structures comprised both nanoscale and microscale features. Droplets on superhydrophobic surfaces can exist in one of two states, nonwetted (droplet rolls off) or wetted (droplet sticks). A fundamental energy barrier exists between these two equilibrium states that is dictated by the surface structures. Nonwetting surfaces promote self-cleaning behaviors and are of great interest for a variety of engineering applications, which makes understanding this energy barrier critical. The self-assembly and metallization of TMV provide a convenient nanofabrication route to create biomimetic structures based on these plants and study their wetting behaviors. Engineered superhydrophobic surfaces were fabricated from SU-8 micropillars coated with TMV-1Cys/Ni and a conformal silane monolayer (Fig. 26); and their static and dynamic wetting properties were characterized.[130] The hydrophobicity was measured by equilibrium contact angle and high-speed imaging during droplet impact. A nanostructured surface without micropillars has the same equilibrium contact angle as the hierarchical micro/nanosurface; however, the wettability of the surface during a water droplet impact is increased for hierarchical surfaces. It was found that the nanoscale and microscale components of the structures were playing two

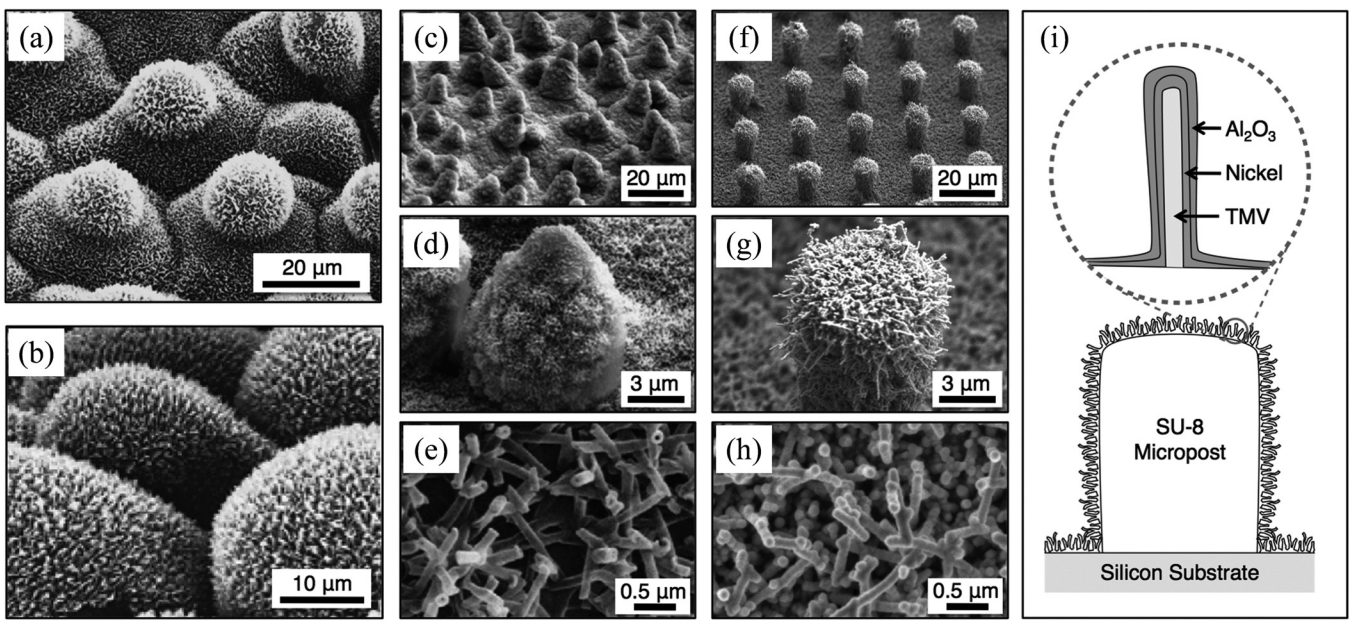

FIG. 26. Superhydrophobic hierarchical plant structures compared to virus-templated biomimetic surfaces. SEM images of the (a) taro plant (*Colocasia esculenta*), (b) parrot feather plant (*Myriophyllum aquaticum*), and (c)–(e) lotus plant (*Nelumbo nucifera*) at various scales. (f)–(h) SEM images of the biomimetic hierarchical structures synthesized for this work using the *Tobacco mosaic virus* assembled onto an array of micropillars at various scales. Reprinted with permission from M. McCarthy, K. Gerasopoulos, R. Enright, J. N. Culver, R. Ghodssi, and E. N. Wang, Appl. Phys. Lett. **100**(10), 5 (2012). Copyright 2012, American Institute of Physics. Note: (a) Reprinted with permission from A. Solga, Z. Cerman, B. F. Striffler, M. Spaeth, and W. Barthlott, Bioinspir. Biomim. **2**(4), S126 (2007). Copyright 2007, IOP Publishing; (b)–(e) Reprinted with permission from K. Koch, B. Bhushan, and W. Barthlott, Prog. Mater. Sci. **54**(2), 137 (2009). Copyright 2009, Elsevier.

distinct roles in repelling impacting droplets. The nanostructures create a large antiwetting capillary pressure due to their small size (ca. 100 nm), while the micropillars disrupt the creation and propagation of large pressures associated with shockwaves generated at the stagnation point during impact. The net result is complete water repellency at impact velocities similar to rainfall. This work lends insight into the evolutionary development of superhydrophobic plant leaves, which require such water repellency to remain nonwetted, thus reducing the growth of harmful bacteria and promoting the uptake of carbon dioxide.

VIII. SUMMARY

In summary, TMV particle geometry can be controlled in sophisticated ways by the chemistry and mechanics of the preparation environment. The ability to combine TMV with inorganic and organic materials produces many exciting composites and hybrid materials that are currently under study. Due to the genetic programmability of TMV coat proteins, the TMV derivatives can be fashioned with enhanced selectivity to analytes, inorganic materials or substrate surfaces. The latter enables effective self-assembly of nanoscale biostructures in functional microdevices. Techniques to position and pattern the TMV-based materials range from stamping to DNA hybridization, ensuring that suitable methods are available for almost any application. In addition, the robustness of the TMV template allows for processing in harsh conditions typically off-limits to biological molecules. Materials based on TMV can derive improved performance from a dramatic increase in surface area. This surface area increase can be amplified by integration with three-dimensional arrays of microelements.

A few examples of the existing functional devices with elements based on TMV include a TMV/ZnO FET, TMV/Ni-Zn microbattery, TMV-based SAW sensor, and TMV-RGD/PVA tissue-engineering scaffold. Some of the applications have already demonstrated virus-enabled enhanced performance on the level of the device components; however, integration of such components into functional systems requires further development. For example, fabrication of a high performance lithium–ion microbattery with 3D hierarchical electrodes requires additional development to combine a solid electrolyte and the second electrode in a sealed package. Successful conjugation of peptides onto the outer surface of TMV is essential for many sensing applications. Development of the methods for precise positioning of TMV-templated nanowires is needed for electronic devices. The next generation of micro/nano/bio systems utilizing functional TMV-based building blocks includes optoelectronic platforms, microfluidics systems, catalyst surfaces with hierarchical architecture, and many others.

The research progress reviewed here is very recent, and it lays a foundation for the further development of this emerging field. We expect novel approaches and developments in the area of virus-assisted fabrication of micro/nano/bio systems in the near future. We believe that the results discussed in this review can inspire engineers and scientists to utilize the *Tobacco mosaic virus* and other related biological particles to improve microdevice performance.

ACKNOWLEDGMENTS

This work was supported by the NSF Nanomanufacturing Program (NSF-CMMI 0927693) and Department of Energy (FG0202ER45975), the Nanostructures for Electrical Energy Storage, an Energy Frontier Research Center funded by the U.S. Department of Energy, Office of Science, Office of Basic Energy Sciences (12DESC0001160), and the Biochemistry Program of the Army Research Office (W911NF1110138). The authors would like to acknowledge the staff at the Maryland Nanocenter clean-room facilities and Nanoscale Imaging Spectroscopy and Properties Lab.

[1]K. Kordas, A. E. Pap, J. Vahakangas, A. Uusimaki, and S. Leppavuori, Appl. Surf. Sci. **252**, 1471 (2005).
[2]J. H. Wang, P. Y. Su, M. Y. Lu, L. J. Chen, C. H. Chen, and C. J. Chu, Electrochem. Solid-State Lett. **8**, C9 (2005).
[3]S. Sun, D. Yang, G. Zhang, E. Sacher, and J.-P. Dodelet, Chem. Mater. **19**, 6376 (2007).
[4]B. Xiang, P. Wang, X. Zhang, S. A. Dayeh, D. P. R. Aplin, C. Soci, D. Yu, and D. Wang, Nano Lett. **7**, 323 (2007).
[5]L. Durrer, T. Helbling, C. Zenger, A. Jungen, C. Stampfer, and C. Hierold, Sens. Actuators B **132**, 485 (2008).
[6]Y. Zhao, J. Jin, and X. Yang, Mater. Lett. **61**, 384 (2007).
[7]X. Feng, K. Shankar, O. K. Varghese, M. Paulose, T. J. Latempa, and C. A. Grimes, Nano Lett. **8**, 3781 (2008).
[8]T. Ghoshal, S. Biswas, S. Kar, A. Dev, S. CHakrabarti, and S. Chaudhuri, Nanotechnology **19**, 065606 (2008).
[9]S. O'Brien, L. Brus, and C. B. Murray, J. Am. Chem. Soc. **123**, 12085 (2001).
[10]X. Wang, X. Wang, W. Huang, P. J. Sebastian, and S. Gamboa, J. Power Sources **140**, 211 (2005).
[11]M. C. Kum, B. Y. Yoo, Y. W. Rheem, K. N. Bozhilov, W. Chen, A. Mulchandani, and N. V. Myung, Nanotechnology **19**, 325711 (2008).
[12]Z. Deng and C. Mao, Nano Lett. **3**, 1545 (2003).
[13]Y. Ma, J. Zhang, G. Zhang, and H. He, J. Am. Chem. Soc. **126**, 7097 (2004).
[14]Y. Hashimoto, Y. Matsuo, and K. Ijiro, Chem. Lett. **34**, 112 (2005).
[15]Q. Gu, C. Cheng, T. Gonela, S. Suryanarayanan, S. Anabathula, K. Dai, and D. T. Haynie, Nanotechnology **17**, R14 (2006).
[16]H. Kudo and M. Fujihira, IEEE Trans. Nanotechnol. **5**, 90 (2006).
[17]J. M. Kinsella and A. Ivanisevic, Langmuir **23**, 3886 (2007).
[18]M. Reches and E. Gazit, Science **300**, 625 (2003).
[19]B. Zhang, S. A. Davis, N. H. Mendelson, and S. Mann, Chem. Commun. **2000**, 781.
[20]R. Mogul, J. J. G. Kelly, M. L. Cable, and A. F. Hebard, Mater. Lett. **60**, 19 (2005).
[21]X. Liang, J. Liu, S. Li, Y. Mei, and W. Yanqing, Mater. Lett. **62**, 2999 (2008).
[22]M. T. Kumara, B. C. Tripp, and S. Muralidharan, J. Phys. Chem. C **111**, 5276 (2007).
[23]D. J. Evans, J. Mater. Chem. **18**, 3746 (2008).
[24]K. Namba, R. K. Pattanayek, and G. R. Stubbs, J. Mol. Biol. **208**, 307 (1989).
[25]R. K. Pattanayek and G. R. Stubbs, J. Mol. Biol. **228**, 516 (1992).
[26]H. Wang and G. R. Stubbs, J. Mol. Biol. **239**, 371 (1994).
[27]H. Wang, J. N. Culver, and G. R. Stubbs, J. Mol. Biol. **269**, 769 (1997).
[28]A. Durham, J. Finch, and A. Klug, Nature **229**, 37 (1971).
[29]W. O. Dawson, D. L. Beck, D. A. Knorr, and G. L. Granthan, Proc. Natl. Acad. Sci. U.S.A. **83**, 1832 (1986).
[30]J. N. Culver, W. O. Dawson, K. Plonk, and G. Stubbs, Virology **206**, 724 (1995).
[31]J. N. Culver, Annu. Rev. Phytopathol. **40**, 287 (2002).
[32]K. Gerasopoulos, M. McCarthy, P. Banerjee, X. Fan, J. N. Culver, and R. Ghodssi, Nanotechnology **21**, 055304 (2010).
[33]E. Royston, S.-Y. Lee, J. N. Culver, and M. T. Harris, J. Colloid Interface Sci. **298**, 706 (2006).
[34]H. Yi *et al.*, Nano Lett. **5**, 1931 (2005).
[35]K. Gerasopoulos, X. Chen, J. Culver, C. Wang, and R. Ghodssi, Chem. Commun. **46**, 7349 (2010).

[36]K. Gerasopoulos, M. McCarthy, E. Royston, J. N. Culver, and R. Ghodssi, J. Micromech. Microeng. **18**, 104003 (2008).
[37]P. A. Machado, H. Fu, R. J. Kratochvil, Y. Yuan, T.-S. Hahm, C. M. Sabliov, C.-I. Wei, and Y. M. Lo, Bioresour. Technol. **101**, 1091 (2010).
[38]H. Fu, P. A. Machado, T. S. Hahm, R. J. Kratochvil, C. I. Wei, and Y. M. Lo, Bioresour. Technol. **101**, 2034 (2010).
[39]K. Gerasopoulos, M. McCarthy, E. Royston, J. N. Culver, and R. Ghodssi, *IEEE MEMS 2008 Conference*, Tucson, AZ, 13–17 January 2008.
[40]J. N. Culver and W. O. Dawson, MPMI **2**, 209 (1989).
[41]X. Z. Fan, K. Gerasopoulos, N. P. Siwak, J. Culver, and R. Ghodssi, IEEE Sensors 2010 Conference, Waikoloa, HI, 1–4 November 2010.
[42]L. A. Lee, H. G. Nguyen, and Q. Wang, Org. Biomol. Chem. **9**, 6189 (2011).
[43]H. Yi, G. W. Rubloff, and J. N. Culver, Langmuir **23**, 2663 (2007).
[44]W. S. Tan, C. L. Lewis, N. E. Horelik, D. C. Pregibon, P. S. Doyle, and H. Yi, Langmuir **24**, 12483 (2008).
[45]M. A. Bruckman, J. Liu, G. Koley, Y. Li, B. Benicewicz, Z. Niu, and Q. Wang, J. Mater. Chem. **20**, 5715 (2010).
[46]C. Yang, A. K. Manocchi, B. Lee, and H. Yi, Appl. Catal., B **93**, 282 (2010).
[47]M. Knez, M. Sumser, A. M. Bittner, C. Wege, H. Jeske, T. P. Martin, and K. Kern, Adv. Funct. Mater. **14**, 116 (2004).
[48]M. Knez, M. Sumser, A. M. Bittner, C. Wege, H. Jeske, S. Kooi, M. Burghard, and K. Kern, J. Electroanal. Chem. **522**, 70 (2002).
[49]M. Knez, A. M. Bittner, F. Boes, C. Wege, H. Jeske, E. Maiβ, and K. Kern, Nano Lett. **3**, 1079 (2003).
[50]A. M. Bittner, X. C. Wu, S. Balci, M. Knez, A. Kadri, and K. Kern, Eur. J. Inorg. Chem. **2005**, 3717.
[51]S. Balci, A. M. Bittner, K. Hahn, C. Scheu, M. Knez, A. Kadri, C. Wege, H. Jeske, and K. Kern, Electrochim. Acta **51**, 6251 (2006).
[52]M. Kobayashi, K. Onodera, Y. Watanabe, and I. Yamashita, Chem. Lett. **39**, 616 (2010).
[53]S. Balci, K. Hahn, P. Kopold, A. Kadri, C. Wege, K. Kern, and A. M. Bittner, Nanotechnology **23**, 045603 (2012).
[54]W. L. Liu, K. Alim, A. A. Balandin, D. M. Mathews, and J. A. Dodds, Appl. Phys. Lett. **86**, 253108 (2005).
[55]M. Ł. Górzny, A. S. Walton, M. Wnęk, P. G. Stockley, and S. D. Evans, Nanotechnology **19**, 165704 (2008).
[56]M. Kobayashi, M. Seki, H. Tabata, Y. Watanabe, and I. Yamashita, Nano Lett. **10**, 773 (2010).
[57]E. Dujardin, C. Peet, G. Stubbs, J. N. Culver, and S. Mann, Nano Lett. **3**, 413 (2003).
[58]R. Tsukamoto, M. Muraoka, M. Seki, H. Tabata, and I. Yamashita, Chem. Mater. **19**, 2389 (2007).
[59]S.-Y. Lee, E. Royston, J. N. Culver, and M. T. Harris, Nanotechnology **16**, S435 (2005).
[60]J.-S. Lim, S.-M. Kim, S.-Y. Lee, E. A. Stach, J. N. Culver, and M. T. Harris, J. Colloid Interface Sci. **342**, 455 (2010).
[61]J.-S. Lim, S.-M. Kim, S.-Y. Lee, E. A. Stach, J. N. Culver, and M. T. Harris, Nano Lett. **10**, 3863 (2010).
[62]J.-S. Lim, S.-M. Kim, S.-Y. Lee, E. A. Stach, J. N. Culver, and M. T. Harris, J. Nanomaterials **2010**, 620505 (2010).
[63]E. Royston, A. Ghosh, P. Kofinas, M. T. Harris, and J. N. Culver, Langmuir **24**, 906 (2008).
[64]A. K. Manocchi, N. E. Horelik, B. Lee, and H. Yi, Langmuir **26**, 3670 (2010).
[65]A. K. Manocchi, S. Seifert, B. Lee, and H. Yi, Langmuir **26**, 7516 (2010).
[66]A. K. Manocchi, S. Seifert, B. Lee, and H. Yi, Langmuir **27**, 7052 (2011).
[67]M. Knez, A. Kadri, C. Wege, U. Gösele, H. Jeske, and K. Nielsch, Nano Lett. **6**, 1172 (2006).
[68]P. Atanasova, D. Rothenstein, J. J. Schneider, R. C. Hoffmann, S. Dilfer, S. Eiben, C. Wege, H. Jeske, and J. Bill, Adv. Mater. **23**, 4918 (2011).
[69]S. Balci *et al.*, Electrochim. Acta **54**, 5149 (2009).
[70]J. E. Crowell, J. Vac. Sci. Technol. A **21**, S88 (2003).
[71]M. Tiitta and L. Niinistou, Chem. Vap. Deposition **3**, 167 (1997).
[72]M. Leskelä and M. Ritala, Angew. Chem., Int. Ed. **42**, 5548 (2003).
[73]O. Sneh, R. B. Clark-Phelps, A. R. Londergan, J. Winkler, and T. E. Seidel, Thin Solid Films **402**, 248 (2002).
[74]S. M. George, Chem. Rev. **110**, 111 (2010).
[75]E. S. Royston, A. D. Brown, M. T. Harris, and J. N. Culver, J. Colloid Interface Sci. **332**, 402 (2009).
[76]X. Chen, K. Gerasopoulos, J. Guo, A. Brown, R. Ghodssi, J. N. Culver, and C. Wang, Electrochim. Acta **56**, 5210 (2011).
[77]X. Chen, K. Gerasopoulos, J. Guo, A. Brown, C. Wang, R. Ghodssi, and J. N. Culver, ACS Nano **4**, 5366 (2010).
[78]X. Chen, J. Guo, K. Gerasopoulos, A. Langrock, A. Brown, R. Ghodssi, J. N. Culver, and C. Wang, J. Power Sources **211**, 129 (2012).
[79]K. Gerasopoulos, E. Pomerantseva, M. McCarthy, A. Brown, C. Wang, J. N. Culver, and R. Ghodssi, ACS Nano **6**, 6422 (2012).
[80]E. Pomerantseva, K. Gerasopoulos, X. Chen, G. Rubloff, and R. Ghodssi, J. Power Sources **206**, 282 (2012).
[81]A. Klug, Philos. Trans. R. Soc. London, Ser. B **354**, 531 (1999).
[82]W. K. Kegel and P. van der Schoot, Biophys. J. **91**, 1501 (2006).
[83]G. Lebeurier, A. Nicolaieff, and K. E. Richards, Proc. Natl. Acad. Sci. U.S.A. **74**, 149 (1977).
[84]Y. Okada, Adv. Biophys. **22**, 95 (1986).
[85]M. R. Falvo, S. Washburn, R. Superfine, M. Finch, F. P. Brooks, Jr., V. Chi, and R. M. Taylor II, Biophys. J **72**, 1396 (1997).
[86]M. A. Bruckman, C. M. Soto, H. McDowell, J. L. Liu, B. R. Ratna, K. V. Korpany, O. K. Zahr, and A. S. Blum, ACS Nano **5**, 1606 (2011).
[87]C. E. Fowler, W. Shenton, G. Stubbs, and S. Mann, Adv. Mater. **13**, 1266 (2001).
[88]Z. Niu, M. A. Bruckman, S. Li, L. A. Lee, B. Lee, S. V. Pingali, P. Thiyagarajan, and Q. Wang, Langmuir **23**, 6719 (2007).
[89]Z. Niu, J. Liu, L. A. Lee, M. A. Bruckman, D. Zhao, G. Koley, and Q. Wang, Nano Lett. **7**, 3729 (2007).
[90]S. P. Wargacki, B. Pate, and R. A. Vaia, Langmuir **24**, 5439 (2008).
[91]S. Balci, D. M. Leinberger, M. Knez, A. M. Bittner, F. Boes, A. Kadri, C. Wege, H. Jeske, and K. Kern, Adv. Mater. **20**, 2195 (2008).
[92]A. Horn, H. G. Schoberth, S. Hiltl, A. Chiche, Q. Wang, A. Schweikart, A. Fery, and A. Boker, Faraday Discuss. **143**, 143 (2009).
[93]A. Schweikart, A. Horn, A. Böker, and A. Fery, Adv. Polym. Sci. **227**, 24 (2010).
[94]A. Mueller, F. J. Eber, C. Azucena, A. Petershans, A. M. Bittner, H. Gliemann, H. Jeske, and C. Wege, ACS Nano **5**, 4512 (2011).
[95]H. Cai, X. Cao, Y. Jiang, P. He, and Y. Fang, Anal. Bioanal. Chem. **375**, 287 (2003).
[96]J. Wang *et al.*, Anal. Chim. Acta **347**, 1 (1997).
[97]K. Srinivasan, *Nanomaterial Sensing Layer Based Surface Acoustic Wave Hydrogen Sensors* (University of South Florida, 2005).
[98]S. V. Kalinin, S. Jesse, W. Liu, and A. A. Balandin, Appl. Phys. Lett. **88**, 153902 (2006).
[99]R. D. Bruin, K. Spelt, J. Mol, R. Koes, and F. Quattrocchio, Nat. Biotechnol. **17**, 397 (1999).
[100]G. Å. Løset, N. Roos, B. Bogen, and I. Sandlie, PLoS One **6**, e17433 (2011).
[101]A. S. Khan, R. Thompson, C. Cao, and J. J. Valdes, Biotechnol. Lett. **25**, 1671 (2003).
[102]P. Samuelson, H. Wernerus, M. Svedberg, and S. Stahl, Appl. Environ. Microbiol. **66**, 1243 (2000).
[103]T. Ide, S. H. Baik, T. Matsuba, and S. Harayama, Biosci. Biotechnol. Biochem. **67**, 1335 (2003).
[104]Z. Han, G. Su, and C. Huang, Sci. China, Ser. C: Life Sci. **42**, 43 (1999).
[105]E. A. Soykut, F. C. Dudak, and I. H. Boyaci, Biochem. Biophys. Res. Commun. **370**, 104 (2008).
[106]H. Ma, B. Zhou, Y. Kim, and K. D. Janda, Toxicon **47**, 901 (2006).
[107]K. A. Kelly, J. Carson, J. R. McCarthy, and R. Weissleder, PLoS One **2**, e665 (2007).
[108]V. A. Petrenko and V. J. Vodyanoy, J. Microbiol. Methods **53**, 253 (2003).
[109]H. B.-Y. Faheng Zang, X. Z. Fan, A. D. Brown, D. L. Kelly, J. N. Culver, and R. Ghodssi, 10th International Workshop on Nanomechanical Sensing (NMC 2013), Stanford, CA, 1–3 May 2013 (unpublished).
[110]A. S. Arico, P. Bruce, B. Scrosati, J.-M. Tarascon, and W. van Schalkwijk, Nature Mater. **4**, 366 (2005).
[111]T. S. Arthur *et al.*, MRS Bull. **36**, 523 (2011).
[112]J. F. M. Oudenhoven, L. Baggetto, and P. H. L. Notten, Adv. Energy Mater. **1**, 10 (2011).
[113]R. Teki, M. K. Datta, R. Krishnan, T. C. Parker, T.-M. Lu, P. N. Kumta, and N. Koratkar, Small **5**, 2236 (2009).
[114]W.-J. Zhang, J. Power Sources **196**, 13 (2011).
[115]M. Armand and J. M. Tarascon, Nature **451**, 652 (2008).
[116]J. M. Tarascon and M. Armand, Nature **414**, 359 (2001).

[117]X. Chen, E. Pomerantseva, P. Banerjee, K. Gregorczyk, R. Ghodssi, and G. Rubloff, Chem. Mater. **24**, 1255 (2012).
[118]X. Chen, E. Pomerantseva, K. Gregorczyk, R. Ghodssi, and G. Rubloff, RSC Adv. **3**, 4294 (2013).
[119]R. J. Tseng, C. Tsai, L. Ma, J. Ouyang, C. S. Ozkan, and Y. Yang, Nat. Nanotechnol. **1**, 72 (2006).
[120]A. Janotti and C. G. Van de Walle, Rep. Prog. Phys. **72**, 126501 (2009).
[121]C.-Y. Chiang, J. Epstein, A. Brown, J. N. Munday, J. N. Culver, and S. Ehrman, Nano Lett. **12**, 6005 (2012).
[122]S. Fujikawa and T. Kunitake, Langmuir **19**, 6545 (2003).
[123]C. L. Lewis, Y. Lin, C. Yang, A. K. Manocchi, K. P. Yuet, P. S. Doyle, and H. Yi, Langmuir **26**, 13436 (2010).
[124]C. Yang and H. Yi, Biochem. Eng. J. **52**, 160 (2010).
[125]C. Yang, A. K. Manocchi, B. Lee, and H. Yi, J. Mater. Chem. **21**, 187 (2011).
[126]L. D. Bolisay, J. N. Culver, and P. Kofinas, Biomacromolecules **8**, 3893 (2007).
[127]P. G. Holder, D. T. Finley, N. Stephanopoulos, R. Walton, D. S. Clark, and M. B. Francis, Langmuir **26**, 17383 (2010).
[128]L. Wu *et al.*, J. Mater. Chem. **21**, 8550 (2011).
[129]M. A. Bruckman, S. Hern, K. Jiang, C. A. Flask, X. Yu, and N. F. Steinmetz, J. Mater. Chem. B **1**, 1482 (2013).
[130]M. McCarthy, K. Gerasopoulos, R. Enright, J. N. Culver, R. Ghodssi, and E. N. Wang, Appl. Phys. Lett. **100**, 263701 (2012).

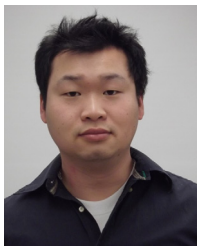

Xiao Zhu Fan is a Ph.D. candidate in the Department of Electrical and Computer Engineering at the University of Maryland. He received both his B.S. (2006) and M.S. (2009) degrees at the University of Maryland, working on microfabricated optical and mechanical sensors. Currently, he is a member of the MEMS Sensors and Actuators Laboratory where his research interests lie in the area of microsensor integration with a focus on biological nanostructures and biofabrication for selective chemical and biological sensing. He is expected to graduate in the summer of 2013.

Ekaterina Pomerantseva is a postdoctoral research associate in the MEMS Sensors and Actuators Laboratory (MSAL) at the Institute for Systems Research, University of Maryland. She received a B.S. degree in Materials Science in 2000 and M.S. degree in Chemistry and Materials Science in 2003 from Lomonosov Moscow State University, a M.S. degree in Biochemistry in 2005 from McGill University, and a Ph.D. degree in Solid-State Chemistry in 2007 from Lomonosov Moscow State University. She was a postdoctoral fellow with Professor Linda Nazar at the University of Waterloo, Canada in 2009–2010 prior to joining Professor Reza Ghodssi at MSAL. Her research interests lie in the development and characterization of novel nanostructured materials for batteries and capacitors to better understand electrochemical energy storage of nanoscale systems and architectures. She has published over 35 journal papers. She will join the Department of Materials Science and Engineering at Drexel University as Assistant Professor in September 2013.

Markus Gnerlich is a Postdoctoral Research Associate with the Institute for Systems Research at the University of Maryland. His current research interests are in solid-electrolyte supercapacitors for high-density flexible integrated circuits and integration of self-assembling nanostructures into microfabrication technology. He received his Ph.D. (2012) and M.S. (2008) in Electrical Engineering from Lehigh University, where he designed, fabricated and tested MEMS force sensors and actuators tailored to liquid environments for cell biophysics experiments. He earned his B.S. (2005) in Electrical Engineering from the Pennsylvania State University with Honors in Bioengineering. While completing his undergraduate degree he spent 3 years working for Xiomedia, a software startup in New York, NY that catered to the financial services industry.

Adam Brown is pursuing a Ph.D. in the Department of Bioengineering at the University of Marlyland. He received a B.S. in Chemistry and Philosophy from Tulane University in 1999. He joined Professor James N. Culver's group as a research assistant in 2007 before joining the laboratory as a graduate student this year. There he worked to develop methods of functionalizing *Tobacco mosaic virus* for energy storage and sensor applications through genetic modification and material coating strategies.

Konstantinos Gerasopoulos received the B.S. degree in Electrical Engineering from the National Technical University of Athens and the M.S. and Ph.D. degrees in Electrical Engineering and Materials Science and Engineering respectively from the University of Maryland, College Park. At Maryland, he was a member of the MEMS Sensors and Actuators Laboratory where he worked on three-dimensional microbattery electrode technologies using nanostructured biomaterials. Dr. Gerasopoulos has worked at TowerJazz Semiconductor in Newport Beach, CA, as a Senior MEMS Process Development Engineer, responsible for the development and ramp to production of MEMS devices for communication applications. He is currently a Research Associate in the Institute for Systems Research at the University of Maryland, College Park. His technical interests include MEMS, semiconductor devices, microfabrication technologies, energy storage devices, and nanostructured materials.

Matthew McCarthy is an Assistant Professor in the Department of Mechanical Engineering and Mechanics at Drexel University in Philadelphia. Prior to joining Drexel he held Postdoctoral appointments in the Department of Mechanical Engineering at the Massachusetts Institute of Technology (2009–2010) and the Department of Electrical and Computer Engineering at the University of Maryland College Park (2007–2008). He received both his M.S. (2004) and Ph.D. (2006) degrees in Mechanical Engineering from Columbia University, working on microfabricated devices and systems for thermal management applications, and his B.S. degree (2002) in Aerospace Engineering from Syracuse University. He is the director of the Drexel Microsystems Laboratory and his research interests are in the areas of micro- and nanoscale structures and systems with a focus on developing micro- and nanofabricated structures, coatings, devices, and systems for enhanced phase-change heat transfer, energy applications, and chemical and biological separations.

James Culver is a Professor in the Institute for Bioscience and Biotechnology and the Department of Plant Sciences and Landscape Architecture at the University of Maryland. He is also affiliated with the Department of Cell Biology and Molecular Genetics, the Fischell Department of Bioengineering, and the Maryland NanoCenter at UMD. Dr. Culver's research is multidisciplinary with efforts directed at understanding virus biology and its role in disease as well as studies aimed at engineering viruses and other biological components for application in nano-based systems and devices. He utilizes a multitude of approaches in these studies and collaborates with scientists in fields ranging from structural biology to microfabrication with the goal of utilizing discoveries in virus biology to develop new approaches for their control and use.

Reza Ghodssi is the Herbert Rabin Distinguished Chair in Engineering, Director of the Institute for Systems Research, and Director of the MEMS Sensors and Actuators Lab in the Department of Electrical and Computer Engineering at the University of Maryland. He is also affiliated with the Fischell Department of Bioengineering, the Maryland NanoCenter, the University of Maryland Energy Research Center, and the Materials Science and Engineering Department at UMD. Dr. Ghodssi's research interests are in the design and development of microfabrication technologies and their applications to micro/nano/bio devices and systems for chemical and biological sensing, small-scale energy conversion and harvesting. Dr. Ghodssi was chair of the NSF Workshop on Micro, Nano, Bio Systems in 2012 and the 9th International Workshop on Micro and Nanotechnology for Power Generation and Energy Conversion Applications known as "PowerMEMS" in 2009. He also served as the Americas Technical Program Committee chair of IEEE SENSORS 2010, 2011, and 2012 conferences. Dr. Ghodssi has over 95 refereed journal publications and is the co-editor of the "MEMS Materials and Processes Handbook" published in 2011.